1

ROYAL AIRCRAFT ESTABLISHMENT

*

Technical Report 79044

April 1979

SKYLAB 1 ROCKET, 1973-27B: ORBIT DETERMINATION AND ANALYSIS

by

D.G. King-Hele

*

Procurement Executive, Ministry of Defence
Farnborough, Hants

UDC 629.19.077.3 : 521.3 : 551.557 : 550.312

ROYAL AIRCRAFT ESTABLISHMENT

(9) Technical Report 79044

Received for printing 24 April 79

(11) (12) 69

(6)

SKYLAB 1 ROCKET, 1973-27B: ORBIT DETERMINATION AND ANALYSIS.

by

(10) D.G. King-Hele (18) DRIC

(14) RAE-TR-79044 (19) ER-68406

SUMMARY

The final-stage rocket which projected Skylab into orbit on 14 May 1973 itself entered a nearly circular orbit at a height near 400 km, inclined at 50° to the equator. The rocket, designated 1973-27B, remained in orbit until 11 January 1975 and, being 25 m long and 10 m in diameter, was the brightest of the artificial satellites then visible. Its orbit has been determined at 62 epochs from some 5000 optical and radar observations. The average orbital accuracy in perigee height and orbital inclination is 90 m, though some orbits with Hewitt camera observations have much smaller sd (down to 10 m).

As the orbit contracted under the influence of air drag, it passed slowly through the 31:2 geopotential resonance, when the track over the Earth repeats every 31 revolutions at intervals of 2 days. The variations in inclination and eccentricity during the resonance phase have been successfully analysed, after some difficulties, and values have been obtained for six lumped 31st-order harmonic coefficients in the geopotential; these will provide a crucial test of the accuracy of future geopotential models.

The variation in inclination before and after resonance has been analysed to determine the average atmospheric rotation rate Λ (rev/day). Results are: $\Lambda = 1.04 \pm 0.05$ at height 380 km between June 1973 and June 1974; $\Lambda = 1.34 \pm 0.09$ at height 305 km for October-December 1974; and $\Lambda = 1.06 \pm 0.06$ at height 200 km in January 1975. A rapid atmospheric rotation at heights of 300-350 km, deduced previously by combining results from many satellites, is thus confirmed by a single satellite.

The observed variations in eccentricity have been compared with those predicted by the (untested) theory for orbit contraction in an atmosphere with strong (threefold) day-to-night variation in density. The comparison confirms the accuracy of the theory and of the *CIRA 1972* atmospheric model.

Departmental Reference: Space 564

LIST OF CONTENTS

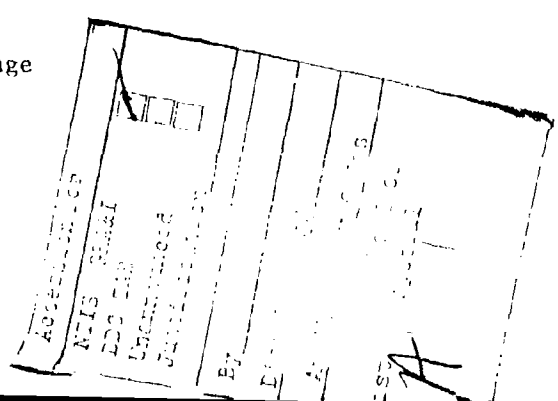

1 INTRODUCTION

The final-stage rocket which fired Skylab 1 into orbit on 14 May 1973 is one of the largest objects ever to have achieved a lengthy orbital life. Designated 1973-27B, it was a 35-ton cylinder[1] with a length of 25 m and a diameter of 10 m, so that its volume exceeded that of Skylab 1 itself. During its 20-month orbital life, which ended on 11 January 1975, the rocket was the brightest of artificial satellites and on an overhead transit was the most brilliant object in the night sky, in the absence of Venus and the Moon.

The orbit was nearly circular and inclined at 50° to the equator. Initially, the average height was 400 km and the orbital period 92.5 minutes. The orbit seemed worthy of analysis because numerous observations were available, and because the orbit passed very slowly through the condition of 31:2 resonance, when the satellite makes 31 revolutions while the Earth spins twice (relative to the orbital plane). Analysis of the orbital perturbations at this resonance offered the chance to obtain values of lumped 31st-order harmonics more accurate than the only others previously obtained[2], from Proton 4, which was not in such a favourable orbit. In addition, the variation in inclination away from resonance was expected to give values for the rotation rate of the upper atmosphere over a wide range of heights; and there was the possibility of testing the theory for the contraction of near-circular orbits in an atmosphere with strong day-to-night variation in density.

2 THE OBSERVATIONS

During its first 15 days in orbit, 1973-27B passed most northern-hemisphere observing stations in the daylight hours, and (apart from a sighting by J. Hewitt and the author on 15 May from Lagonissi in Greece) the only observations available were two from Sydney, Australia, and observations on 8 transits from the radar at RSRE Malvern - not enough to allow the determination of unbiased orbits.

From June 1973 onwards, daily US Navy observations from the Navspasur system were available*, and orbits could have been determined at any chosen time. Continuous orbit determination was not necessary for 1973-27B, however, except at the time of the 31:2 resonance and at the end of the life, so the policy adopted was to determine orbits whenever there were appreciable numbers of other observations in addition to the US Navy observations. About 1500 of the US Navy observations were used, while the 'other observations' fell into five categories, as follows.

* Navspasur observations were being made in May, of course, but were not requested until June.

First, and most accurate, were 28 transits recorded by the Hewitt cameras at Malvern (27 transits) and Edinburgh (1 transit), with accuracies between 1 and 3 seconds of arc. A maximum of 5 observations per transit was used, although on some transits only one or two observations were available.

Second in order of accuracy was the kinetheodolite at the South African Astronomical Observatory. These observations, of accuracy between 30 and 100 seconds of arc, were available on 69 transits, usually with 2 observations per transit, and had a profound influence on the values of the orbital parameters, because of the accuracy of the observations and the sparsity of other southern-hemisphere data.

The third and largest group of 'other observations', over 1400, came from volunteer visual observers reporting to the Appleton Laboratory at Slough or the Moonwatch Division of the Smithsonian Astrophysical Observatory. For the majority of these observations the accuracies were between 1 and 4 minutes of arc cross-track.

The fourth group of observations was from the radar tracker at RSRE Malvern. Observations were available on 82 transits and a maximum of 3 observations per transit was used, although sometimes only one was available. The average accuracy was about 1 km in range and 3 minutes of arc in direction.

The fifth group consisted of more than 1000 observations in the last 7 days of the satellite's life, provided by the assigned and contributing sensors of the North American Air Defense Command (NORAD) Space Detection and Tracking System (SPADATS). With these observations, and the US Navy and Malvern radar observations, it was possible to determine 6 excellent orbits at daily intervals at the end of the life.

3 THE ORBITS

3.1 General

The orbits were determined using the PROP6 orbit refinement program[3,4], in which each observation is given an *a priori* error, and the program proceeds by an iterative process to reduce the measure of fit, c, where c^2 is defined as the sum of the squares of the weighted residuals, divided by the number of degrees of freedom. The weighted residual is the residual in right ascension or declination, divided by the *a priori* error. If the orbit fits the observations well, the value of c should be somewhat less than 1, because the *a priori* errors are normally taken as round-number values somewhat higher than the actual errors. In the orbit refinement process, any observations with weighted residuals greater than 3σ are rejected.

The orbit of 1973-27B proved unexpectedly difficult to determine, chiefly because an excessive number of observations were rejected. Two reasons for this difficulty are now apparent. First, the brightness of 1973-27B enticed into action a large number of new visual observers, whose accuracy did not match their enthusiasm; in retrospect it would have been more efficient not to have used any of their observations. (The experienced visual observers gave realistic estimates of their accuracy, as usual.) Second, nearly all the observations were less accurate than usual, because of the satellite's large size, great brightness and high apparent angular rate of travel (see section 4). Over all, about 25% of the observations were rejected.

3.2 Accuracy of the orbital parameters

Orbits were determined at 62 epochs between 17 June 1973 and 11 January 1975. In the first year, before the 31:2 resonance began to take effect, orbits were determined whenever there were substantial numbers of other observations to support the US Navy observations: orbits were calculated at 27 epochs during these 12 months, and US Navy observations at elevations less than 20° were not used. During the months when resonance effects were appreciable (1 July to 10 October 1974), as many orbits as possible (17) were determined, and the low elevation US Navy observations were included. Between 16 October 1974 and decay, the procedure reverted to the less intensive mode, and 18 orbits were determined, including the 6 daily orbits in the last 6 days. The values of the orbital parameters are listed in Table 1 (pages 43-45).

The accuracy of the orbits varied a great deal, the presence or absence of Hewitt camera or kinetheodolite observations being a decisive factor. On 16 of the 18 orbits with Hewitt camera observations, the standard deviation in inclination i was between 0.0001° and 0.0007°, with a mean of 0.0004° (equivalent to 50 m in position). On 15 of these 18 orbits, the standard deviation in eccentricity e ranged between 4 and 15×10^{-6}, with an average of 10×10^{-6}, equivalent to 70 m in perigee distance; the standard deviation in right ascension of the node Ω was 0.002° or less on all 18 orbits.

On 40 of the 44 orbits without Hewitt camera observations, the standard deviation in inclination ranged between 0.0005° and 0.0016°, with an average of 0.0010°, equivalent to 120 m in distance. (The remaining four orbits, for which observations were deficient in either number or variety, had accuracies between 0.0018° and 0.0025°.) On 40 of the 44 orbits, the standard deviation in eccentricity ranged from 5 to 21×10^{-6}, with a mean of 12×10^{-6}, equivalent to 80 m in perigee height; and the average standard deviation in Ω was less than 0.002°.

Thus the presence of Hewitt camera observations improves the sd in inclination by a factor of 2.5, but in eccentricity by a factor of only 1.2: for accurate values of eccentricity, a wide geographical distribution of observations is more important than very accurate observations from one site, and the Cape kinetheodolite, because of its geographical advantage, was often just as influential as the Hewitt camera in determining e.

Within PROP, the mean anomaly M is expressed as a polynomial in time t, of the form

$$M = M_0 + M_1 t + M_2 t^2 + \ldots M_5 t^5 \quad , \qquad (1)$$

where t is the time in days after epoch, M_0 is the value of M at epoch, and $M_2 \ldots M_5$ are coefficients which are included if they are needed. With 19 of the orbits, only M_0, M_1 and M_2 were required: this implies that the drag remained nearly constant during the time interval covered by the observations. On the remaining orbits larger numbers of M-coefficients were needed, as a result of variations in density. The density at heights near 240 km during 1973 and 1974 has been determined by Walker[5] at average intervals of about 2 days: irregular day-to-day variations of up to about 20% often occur, and the amplitude of such variations would be larger at the heights being sampled by 1973-27B during its first year in orbit (350-400 km). The density at these heights at weekly intervals during 1974 has been determined by Brookes and Moore[6] from analysis of the orbit of 1973-27A.

The use of numerous M-coefficients is not to be recommended, because of their possible correlations with other parameters. Here an extra M-coefficient has been used only if: (a) the value of the measure of fit ϵ is reduced by at least 20%; (b) the standard deviations of the main orbit parameters are reduced; and (c) the value of the new M-coefficient is at least 5 times its standard deviation. The ingredients of a good orbit - exemplified by No. 8 - are (i) having accurate observations, well distributed geographically, and (ii) fitting with M_0, M_1 and M_2 only, preferably with a low value of M_2.

The values of M_1 and M_2 are of course very well-determined on all the orbits, M_1 being accurate to 1 part in 10^6 (except on the last orbit) and M_2 to 1 part in 100 (except on orbits 4, 26 and 28).

For most of the orbits, changes in the assumed value for the density scale height H had a negligible effect, and H was taken as 50 km. The effect of H was appreciable only on the last four orbits, when the perigee heights were

201, 193, 180 and 158 km respectively, and values of H were taken as 30, 29, 26 and 20 km respectively, in accordance with the COSPAR International Reference Atmosphere 1972 (Ref 7).

Table 1 shows the wide variation in the number of observations per orbit, between 20 and 98, with a mean of 45. The time intervals covered by the observations range between 1 day (for the last 6 orbits) and 9 days, with a mean of 5 days. The values of ε (except on orbit 57) were between 0.40 and 0.88, which is very satisfactory.

The last six (daily) orbits were of excellent accuracy and consistency. The satellite burnt up near the Azores at 07.05 UT on 11 January 1975, so the epoch of the final orbit is only 7 hours before decay. Two US Navy observations at 05.59 UT were, not surprisingly, rejected by PROP, and their sd was artificially increased (to about 10 km) to ensure that they were used in the final orbit, to strengthen the values of the M-coefficients.

3.3 Variation of the orbital parameters

The values of inclination on the 62 orbits of Table 1, with their standard deviations, are plotted in Fig 1. The general decrease due to the effect of atmospheric rotation is visible, with a hint of an increase at the time of the 31:2 resonance; but the values are rather scattered, and no conclusions can be drawn until the lunisolar, zonal harmonic and $J_{2,2}$ perturbations are removed (see section 5).

The 62 values of eccentricity are plotted in Fig 2, their standard deviations being too small to indicate. Fig 2 shows clearly the oscillation due to odd zonal harmonic perturbations, which is of amplitude 0.8×10^{-3}, together with the general decrease in eccentricity due to air drag. The points have been joined by a broken curve as a guide to the eye. Any perturbation due to the 31:2 resonance must be very small compared with the major perturbations due to zonal harmonics and air drag.

Fig 3 gives an alternative plotting of the eccentricity, using e and the argument of perigee ω as polar coordinates. In the absence of drag, the locus of the points would be a circle with its centre at the point C on the $e \sin \omega$ axis: the action of drag converts the circle into a decaying spiral. The day-to-night variation in air density displaces the centre of the spiral from the $e \sin \omega$ axis[8], but this is scarcely perceptible in Fig 3, where the spiral is of classic regularity until the last few days in orbit. (The variation of e and ω in these last days is discussed in section 8.3.)

Fig 4 shows the values of the right ascension of the node, which decreases smoothly and almost linearly, at a rate of 5.2 deg/day initially, increasing to 5.9 deg/day on the final orbit.

Fig 5 gives the values of the orbital decay rate M_2. As time passes, the satellite gradually sinks lower into the atmosphere, and there is a general increase in the decay rate. The values also reflect the semi-annual variation in air density[5], with minima of M_2 in August 1973 and January 1974, separated by maxima in October 1973 and March 1974. The minimum in July 1974 is just visible, but the massive increase in September-October 1974 is caused mainly by the decreasing height of the satellite.

4 ANALYSIS OF THE OBSERVATIONS

The residuals of the observations utilized in orbits 1-56 have been listed with the aid of the ORES program[9], and have been sent to the observers. Table 2 gives the rms residuals for the stations (in nine different countries) having five or more observations accepted. The angular residuals for Station 29 are geocentric, and need to be multiplied by a factor of about 5 to make them comparable with the other (topocentric) values. The residuals for observations on the last six orbits are not given.

The residuals in Table 2 are generally rather larger than in other recent orbit determinations, using similar observations[10-12]. One likely reason is that 1973-27B often moved rapidly (at 1 deg/s or more) relative to the star background: such rapid motion increases the angular error resulting from timing errors. The Hewitt camera at Malvern, which has very accurate timing, is unaffected by the rapid motion, and the total rms residual for the camera is only 2 seconds of arc, as usual. But for the visual observers the timing errors when observing 1973-27B (about 100 ms) were more important than angular errors, and the along-track residuals usually exceeded the cross-track residuals. This tendency is visible in Table 2 for the British observers, who often made their observations of 1973-27B when it was at high elevation in the south and was travelling from west to east: in these circumstances the along-track errors are mainly in right ascension, and the right ascension residuals are on average about twice those in declination for the seven British observers with the most observations accepted - Stations 2420, 2414, 2421, 2265, 2419, 2430 and 2428. The declination residuals therefore give a better idea of the angular accuracy of the observers, and, since the rms residuals tend to be unduly influenced by one poor observation, it is fair to say that in good conditions the visual observers should be capable of an angular accuracy about half the rms declination residuals

in Table 2. (The relation between rms residuals and the average in best conditions has been discussed in section 5 of Ref 13.)

Table 2

Residuals of the observations on orbits 1-56, for stations with 5 or more observations accepted

Station		Number of observations accepted	Rms residuals			
			Range	Minutes of arc		
			km	RA	Dec	Total
1	US Navy	143		2.2	2.3	3.2
2	US Navy	23		2.5	3.0	3.9
3	US Navy	40		1.7	1.6	2.3
4	US Navy	36		1.6	1.9	2.5
5	US Navy	35		2.1	2.1	3.0
6	US Navy	78		2.2	2.3	3.2
29*	US Navy	987	0.6	0.4	0.4	
86 & 2597	Rodental	15		5.1	3.0	5.9
161	Castlerock	5		1.8	1.1	2.1
414	Capetown	44		3.3	4.1	5.3
614	Thallon	9		3.9	4.0	5.6
719	Rodewisch	22		5.0	3.4	6.0
759	Cluj	8		1.8	4.7	5.0
2265	Farnham	37		4.0	2.1	4.6
2303	Malvern camera	90		0.03	0.02	0.04
2304	Malvern radar	149	1.3	4.4	2.8	
2414	Bournemouth	108		5.7	3.0	6.4
2419	Tremadoc	30		4.8	2.6	5.4
2420	Willowbrae	134		4.6	1.5	4.8
2421	Malvern 4	78		3.6	2.5	4.4
2428	Frimley	19		6.0	3.3	6.8
2430	Stevenage 4	20		4.0	2.0	4.5
2528	Aldershot	16		2.6	3.0	4.0
2539	Dymchurch	5		3.5	1.8	3.9
2573	Genoa 1	14		8.6	16.1	18.3
2577	Cape kinetheodolite	96		1.2	1.3	1.7
2596	Akrotiri	21		4.2	4.6	6.2
4126	Groningen	10		2.2	1.5	2.7
4130	Denekamp	15		4.8	4.7	6.7
4156	Apeldoorn	15		5.7	3.5	6.7
4159	Achel 2	5		4.3	6.7	8.0
4165	Groningen 3	5		5.2	5.3	7.4
8517	Sacramento 1	23		5.3	4.8	7.1
	Others	85				
	Total	2420				

* Geocentric

It is also probable that the accuracy of the visual observers was adversely affected by the extreme brightness of the satellite, which was sometimes of magnitude -2. Reference stars were often lost in the glare as the satellite passed them, a situation scarcely conducive to good accuracy. This difficulty, aggravated by the high angular velocity of the satellite (often more than 1° per second), proved too much for some of the inexperienced visual observers, and only 743 of the original 1400 visual observations were accepted in the final orbits. Of these, 18% were from Willowbrae (R.D. Eberst), 15% from Bournemouth (D.J. Hopkins), 10% from Malvern 4 (D.M. Brierley), 6% from Cape Town (W.P. Hirst), 5% from Farnham (D.G. King-Hele) and 4% from Tremadoc (D.C. Mason). Thus 58% of the accepted visual observations came from only 6 observers - a pattern familiar in many previous orbit determinations[10-12].

The US Navy and Malvern radar observations, for which timing is by electronic methods, also have rather larger residuals than usual: probably the errors were increased because the satellite was so large that it produced multiple radar reflections.

The kinetheodolite observations were also less accurate than usual. There are two possible reasons: first, the unusually rapid angular tracking rates needed on transits at high elevations might have had a bad effect; second, and rather paradoxically, the clear skies of South Africa and the brightness of the satellite combined to allow an exceptional number of observations at very low elevation, often less than 10°, for which errors in the atmospheric refraction correction would be larger (see section 5).

5 REVISION OF THE ORBITS

When lunisolar, zonal harmonic and $J_{2,2}$ perturbations have been removed, the values of inclination (outside the 31:2 resonance region) should lie on a smooth curve, slowly decreasing under the influence of atmospheric rotation. (The effects of other perturbations, such as Earth and ocean tides[14], are expected to be less than the standard deviations of the values, and are ignored.)

With the orbits originally computed, however, the values of inclination, after removal of perturbations, did not lie on a smooth curve, but were quite scattered. The theoretical curves for various atmospheric rotation rates Λ were calculated, and a value $\Lambda = 1.0$ between launch and resonance seemed to fit the scattered values best: after some trial-and-error experiments with orbits 1-7, a mean curve was established, with $\Lambda = 1.0$. On the assumption that the mean curve was more likely to give the correct value of i than the scattered orbits, any orbit between No.8 and No.27 that did not fit the curve was re-run

with the inclination fixed at the value indicated by the curve. Any observations which could not tolerate this inclination were then omitted - with the exception of the Cape kinetheodolite observations, for which the *a priori* error was doubled if the observation was rejected or had a large residual. The orbit was then again re-run, with the inclination free. On most occasions, the revised orbit thus obtained had both a lower value of ϵ and lower standard deviations than the original orbit, as well as an inclination closer to the mean curve: this is a strong indication that the non-conforming observations were in error. (If ϵ was not reduced, the new orbit was not accepted.) A similar procedure was applied after resonance. It is of course these revised orbits that are given in Table 1 and Fig 1, and, when the perturbations are removed, the values of inclination decrease quite smoothly, as Fig 6 shows, except near resonance.

It may seem disquieting that such refinement is needed: the need arises because of the vulnerability of least-squares fitting to the influence of observations which are in error by two or three times their pre-assigned accuracy. Omitting such an observation can change the value of i by several standard deviations. 'Wrong' observations are often very difficult to identify, however - especially if isolated geographically - when fitting a changing orbit to the motion of a satellite decaying under the action of variable air drag. To reduce the rejection level to less than 3ϵ would be to risk rejecting good observations, and a rejection level differing between one orbit and another would be difficult to justify. So the technique of introducing independent information about the likely value of inclination seems not only legitimate and logical, but quite essential, if the dilemma is to be resolved*.

For 1973-27B, the problem can be seen in retrospect as largely stemming from overweighting of the Cape kinetheodolite observations. These have a greater influence than any other observations, because they are often both geographically isolated and more accurate than any others (in the absence of Hewitt camera observations). In the original orbits the accuracy of the kinetheodolite observations was taken as 0.01° whenever this was the figure specified by the observers. It would have been wiser to have used 0.02°, for several reasons.

---

* Though the least-squares method has its virtues, orbit determination tends to expose its weaknesses. Godwin said of Parliament, "To decide truth by the casting up of numbers is an intolerable insult to reason". To decide that 'truth' is revealed by the exact location of a shallow minimum in a nearly flat multidimensional surface may also seem an insult, when the removal of only one observation can so alter the surface that the minimum may be displaced by an amount much greater than the formal sd. It seems unlikely that other methods can do much better, however, because there is no sure way of defining a 'bad' observation.

First, although 0.01° is a fair 'round-number' accuracy estimate, the average error of these observations is probably rather larger, perhaps about 0.013°. Second, all the other observations are given pessimistic *a priori* accuracies - that is why the values of ϵ are usually between 0.5 and 0.8 - and it is bad practice to give heavier relative weighting to isolated observations. Third, there are some doubts about the accuracy of the station coordinates for the kinetheodolite, which would argue for an error larger than 0.01° for high-elevation observations. Fourth, as mentioned in section 4, many of the kinetheodolite observations of 1973-27B were made at very low elevations, where the larger errors in the refraction correction might vitiate the assumption of an accuracy of 0.01°. For these reasons, it is recommended that an accuracy of 0.02° should be used for the Cape kinetheodolite observations in future orbit determinations: this will ensure that future observations will not be lost through rejection (a loss that can be ill afforded); and fewer orbits will be disturbed by the minority of observations that would otherwise have been overweighted.

6 THE 31:2 RESONANCE

6.1 General

The orbit of 1973-27B experienced the effects of 31:2 resonance between July and October 1974. Exact 31:2 resonance occurred on 23 August 1974 (MJD 42282). The raw values of inclination in Fig 1 give a hint of an increase in inclination at the time of the resonance, and this emerges more clearly when the perturbations are removed, as in Fig 6. Any variations in eccentricity due to resonance are masked in Fig 2 by the larger variations due to odd zonal harmonics and air drag. The removal of these effects is difficult, and is discussed in section 6.4.

6.2 Theory

The longitude-dependent part of the Earth's gravitational potential at an exterior point (r, θ, λ) may be written in normalized form[15] as

$$\frac{\mu}{r} \sum_{\ell=2}^{\infty} \sum_{m=1}^{\ell} \left(\frac{R}{r}\right)^{\ell} P_{\ell}^{m}(\cos\theta) \left\{ \bar{C}_{\ell m} \cos m\lambda + \bar{S}_{\ell m} \sin m\lambda \right\} N_{\ell m} , \qquad (2)$$

where r is the distance from the Earth's centre, θ is co-latitude, λ is longitude (positive to the east), μ is the gravitational constant for the Earth ($398600\ km^3/s^2$), R is the Earth's equatorial radius (6378.1 km), $P_{\ell}^{m}(\cos\theta)$ is

the associated Legendre function of order m and degree ℓ, and $\bar{C}_{\ell m}$ and $\bar{S}_{\ell m}$ are the normalized tesseral harmonic coefficients. The normalizing factor $N_{\ell m}$ is given by[15]

$$N_{\ell m}^2 = \frac{2(2\ell + 1)(\ell - m)!}{(\ell + m)!} \quad . \tag{3}$$

When a satellite orbit experiences $\beta{:}\alpha$ resonance - that is, when the satellite makes β revolutions while the Earth makes α revolutions relative to the satellite's orbital plane - the rates of change of inclination and eccentricity depend on the resonance angle Φ, defined by

$$\Phi = \alpha(\omega + M) + \beta(\Omega - \nu) \ , \tag{4}$$

where ν is the sidereal angle. The perturbation produced in i and e by a relevant pair of harmonic coefficients, $\bar{C}_{\ell m}$ and $\bar{S}_{\ell m}$, may be written[16,17]

$$\frac{di}{dt} = \frac{n(1 - e^2)^{-\frac{1}{2}}}{\sin i} \left(\frac{R}{a}\right)^{\ell} \bar{F}_{\ell mp} G_{\ell pq} (k \cos i - m) \Re\left[j^{\ell - m + 1} \left(\bar{C}_{\ell m} - j\bar{S}_{\ell m}\right) \exp\left\{j(\gamma\Phi - q\omega)\right\}\right], \tag{5}$$

$$\frac{de}{dt} = n\left(1 - e^2\right)^{-\frac{1}{2}} \left(\frac{R}{a}\right)^{\ell} \bar{F}_{\ell mp} G_{\ell pq} \left\{\frac{q - \frac{1}{2}(k + q)e^2}{e}\right\} \Re\left[j^{\ell - m + 1} \left(\bar{C}_{\ell m} - j\bar{S}_{\ell m}\right) \exp\left\{j(\gamma\Phi - q\omega)\right\}\right] \ . \tag{6}$$

Here $\bar{F}_{\ell mp}$ is Allan's normalized inclination function[16], $G_{\ell pq}$ is a function of eccentricity e for which explicit forms have been derived by Gooding[17], $\Re$ denotes 'real part of' and $j = \sqrt{-1}$. The indices γ, p, k and p are integers, with γ taking the values 1, 2, 3, ..., and q the values 0, ±1, ±2, ... The equations linking ℓ,m,k and p are[17]: $m = \gamma\beta$; $k = \gamma\alpha - q$; $2p = \ell - k$.

For a particular $\beta{:}\alpha$ resonance, the relevant value of m in the $\bar{C}_{\ell m}$, $\bar{S}_{\ell m}$ coefficients is decided by the choice of γ, since $m = \gamma\beta$. There is a series of possible values of ℓ - any values such that $\ell \geq m$ and $(\ell - k)$ is even. The successive $\bar{C}_{\ell m}$, $\bar{S}_{\ell m}$ coefficients that arise (for given γ and q) may usefully be combined in 'lumped' form and written as

$$\bar{C}_m^{q,k} = \sum_{\ell} Q_{\ell}^{q,k} \bar{C}_{\ell m} \ , \qquad \bar{S}_m^{q,k} = \sum_{\ell} Q_{\ell}^{q,k} \bar{S}_{\ell m} \ , \tag{7}$$

where ℓ increases in steps of 2 from its minimum permissible value ℓ_0 ; the $Q_\ell^{q,k}$ are functions of inclination that can be taken as constant for a particular satellite; and $Q_\ell^{q,k} = 1$ when $\ell = \ell_0$.

Here, with $B = 31$ and $\alpha = 2$, the relevant harmonics are of order $m = 31\gamma$, where $\gamma = 1, 2, 3, \ldots$. The harmonics of order 62, 93, ..., are unlikely to have much influence, and, although their effects need to be tested, only the $\gamma = 1$ terms (that is, the effects of harmonics of order $m = 31$) will be given explicitly.

Also, since $k = 2 - q$ if $\gamma = 1$, the values of $(\ell - k)$ are even if $(\ell + q)$ is even: so the relevant values of ℓ are those for which $(\ell + q)$ is even and $\ell \geq 31$.

As pointed out by Walker[10], the $q = 0, \pm 1, \pm 2, \ldots$, terms in the expression (5) for di/dt have G coefficients of order 1, $\frac{1}{2}\ell e$, $\frac{1}{8}(\ell e)^2$ ... since the $G_{\ell pq}$ are[17] of order $\dfrac{(\frac{1}{2}\ell e)^{|q|}}{(|q|)!}$. For 1973-27B, e is of order 0.03, so $\frac{1}{2}\ell e \sim 0.1$ for $\ell \sim 60$, and only the $q = 0$ terms are likely to affect the variation of i . The situation is different with the perturbation in e , because in equation (6) the term $\frac{1}{e} G_{\ell pq}\left\{q - \frac{1}{2}(k + q)e^2\right\}$ is of order e for $q = 0$; of order $\frac{1}{2}\ell$ for $q = \pm 1$; of order $\frac{1}{4}\ell^2 e$ for $q = \pm 2$; of order $\frac{1}{16}\ell^3 e^2$ for $q = \pm 3$; ... . With $e \sim 0.003$, only the $q = \pm 1$ terms are likely to affect the variation of eccentricity.

So, when fitting theoretical curves to the variations of i and e at resonance for 1973-27B, it is probable that the only terms needed will be those with $(\gamma, q) = (1, 0)$ for inclination, and $(\gamma, q) = (1, 1)$ and $(1, -1)$ for eccentricity. Explicit forms for di/dt and de/dt in terms of these three (γ, q) pairs have been given in Ref 2. Here it is only necessary to quote explicitly the $(\gamma, q) = (1, 0)$ terms for di/dt ,

$$\frac{di}{dt} = \frac{n}{\sin i}\left(\frac{R}{a}\right)^{32}\left[(31 - 2\cos i)\bar{F}_{32,31,15}\left\{\bar{S}_{31}^{0,2}\sin\Phi + \bar{C}_{31}^{0,2}\cos\Phi\right\}\right.$$

$$\left. + \text{terms in } e^{|q|}\begin{matrix}\cos\\ \sin\end{matrix}(\gamma\Phi - q\omega)\right] , \quad (8)$$

and the $(\gamma, q) = (1, \pm 1)$ terms for de/dt ,

$$\frac{de}{dt} = n\left(\frac{R}{a}\right)^{31}\Big[-17\bar{F}_{31,31,15}\left\{\bar{C}_{31}^{1,1}\sin(\Phi-\omega) - \bar{S}_{31}^{1,1}\cos(\Phi-\omega)\right\} + 13\bar{F}_{31,31,14}\left\{\bar{C}_{31}^{-1,3}\sin(\Phi+\omega) - \bar{S}_{31}^{-1,3}\cos(\Phi+\omega)\right\} + \text{terms in } e^{|q|-1}(q-\gamma e^2)\begin{matrix}\cos\\ \sin\end{matrix}(\gamma\Phi - q\omega)\Big] \quad . \tag{9}$$

In equations (8) and (9), the value of Φ is, from equation (4), given by

$$\Phi = 2(\omega + M) + 31(\Omega - \nu) \quad . \tag{10}$$

The values of Φ and $\dot{\Phi}$ for 1973-27B between July and October 1974 are plotted in Fig 7.

The lumped C and S coefficients in equations (8) and (9) may be written in terms of the $\bar{F}_{\ell mp}$ and R/a as follows:

$$\bar{C}_{31}^{0,2} = \bar{C}_{32,31} - \frac{\bar{F}_{34,31,16}}{\bar{F}_{32,31,15}}\left(\frac{R}{a}\right)^2\bar{C}_{34,31} + \frac{\bar{F}_{36,31,17}}{\bar{F}_{32,31,15}}\left(\frac{R}{a}\right)^4\bar{C}_{36,31} - \ldots \tag{11}$$

$$\bar{C}_{31}^{1,1} = \bar{C}_{31,31} - \frac{18\bar{F}_{33,31,16}}{17\bar{F}_{31,31,15}}\left(\frac{R}{a}\right)^2\bar{C}_{33,31} + \frac{19\bar{F}_{35,31,17}}{17\bar{F}_{31,31,15}}\left(\frac{R}{a}\right)^4\bar{C}_{35,31} - \ldots \tag{12}$$

$$\bar{C}_{31}^{-1,3} = \bar{C}_{31,31} - \frac{14\bar{F}_{33,31,15}}{13\bar{F}_{31,31,14}}\left(\frac{R}{a}\right)^2\bar{C}_{33,31} + \frac{15\bar{F}_{35,31,16}}{13\bar{F}_{31,31,14}}\left(\frac{R}{a}\right)^4\bar{C}_{35,31} - \ldots \tag{13}$$

and similarly for S , on replacing C by S throughout. The numerical values of the lumped coefficients for 1973-27B, at inclination 50.04°, are

$$\bar{C}_{31}^{0,2} = \bar{C}_{32,31} - 7.4\bar{C}_{34,31} + 27.6\bar{C}_{36,31} - 62.4\bar{C}_{38,31} + 89.0\bar{C}_{40,31} - 71.1\bar{C}_{42,31} + 7.5\bar{C}_{44,31} + 45.2\bar{C}_{46,31} - 33.1\bar{C}_{48,31} - 17.1\bar{C}_{50,31} + 31.4\bar{C}_{52,31} + 3.0\bar{C}_{54,31} - 24.6\bar{C}_{56,31} + 2.5\bar{C}_{58,31} + 18.4\bar{C}_{60,31} - \ldots . \tag{14}$$

$$\bar{C}_{31}^{1,1} = \bar{C}_{31,31} - 15.6\bar{C}_{33,31} + 92.8\bar{C}_{35,31} - 316.3\bar{C}_{37,31} + 692.2\bar{C}_{39,31} - 979.6\bar{C}_{41,31}$$
$$+ 784.4\bar{C}_{43,31} - 64.0\bar{C}_{45,31} - 561.7\bar{C}_{47,31} + 428.5\bar{C}_{49,31} + 215.5\bar{C}_{51,31}$$
$$- 441.2\bar{C}_{53,31} - 15.0\bar{C}_{55,31} + 363.1\bar{C}_{57,31} - 72.9\bar{C}_{59,31} - \ldots \quad \ldots.(15)$$

$$\bar{C}_{31}^{-1,3} = \bar{C}_{31,31} - 12.8\bar{C}_{33,31} + 61.9\bar{C}_{35,31} - 165.9\bar{C}_{37,31} + 268.7\bar{C}_{39,31} - 239.9\bar{C}_{41,31}$$
$$+ 35.7\bar{C}_{43,31} + 161.5\bar{C}_{45,31} - 126.3\bar{C}_{47,31} - 70.6\bar{C}_{49,31} + 129.1\bar{C}_{51,31}$$
$$+ 20.3\bar{C}_{53,31} - 110.6\bar{C}_{55,31} + 1.7\bar{C}_{57,31} + 91.1\bar{C}_{59,31} - \ldots \quad \ldots.(16)$$

and similarly for S. Equations (14)-(16) show that, if good values for the lumped coefficients can be found, they will provide a stringent test of the accuracy of future geopotential models with coefficients to degree 60 or more.

6.3 Analysis of inclination

The analysis begins 50 days before exact resonance, at MJD 42232 when $\dot{\Phi} = -26.4$ deg/day, and ends 48 days beyond resonance, at MJD 42330, when $\dot{\Phi} = 42.9$ deg/day. As Fig 7 shows, $\dot{\Phi}$ increases more rapidly after resonance than before, because of an increase in the orbital decay rate, resulting from the satellite's decreasing height and the semi-annual increase in air density between August and October.

The values of inclination were cleared of zonal-harmonic and lunisolar perturbations by using the PROD computer program[18] with 1-day integration step; the perturbations due to the $J_{2,2}$ tesseral harmonic, which are recorded with each PROP orbit, were also removed. The resulting values of i in the resonance region were fitted using the THROE computer program[19] with $(\gamma, q) = (1, 0)$. In these computations the value of M_2 on orbit n, at epoch t_n, was replaced by

$$\bar{M}_2 = \frac{(M_1)_{n+1} - (M_1)_n}{2(t_{n+1} - t_n)} ,$$

because the numerical integration within THROE proceeds on the assumption that M_2 remains constant between time t_n and time t_{n+1}. The use of $\bar{M}_2$ ensures that THROE correctly models the total change in M_1 due to drag between orbit n and orbit $(n + 1)$.

The first THROE run using the 17 orbits with an atmospheric rotation rate Λ = 1.2 rev/day gave encouraging results: the measure of fit ϵ was 1.03 and the values of $10^{6-0,2}C_{31}$ and $10^{6-0,2}S_{31}$ were 0.4 ± 0.6 and -1.0 ± 0.4. However, several of the orbits fitted badly, and a process of revision was started, similar to that described in section 5. The effects of changing the density scale height H and the rotation rate Λ were also assessed. Alteration of H had little effect: the value chosen, H = 45 km, was that obtained[7] from *CIRA 1972* for the appropriate average level of solar activity, and average local time, at a height of 350 km, 0.4H above the mean perigee height[20]. For the rotation rate Λ, previous results[21] indicate a mean value of 1.3 at a height of 350 km, and since THROE revealed a slightly (0.4%) better fit with Λ = 1.3 than with Λ = 1.2, the higher value was adopted.

In the final THROE run, with the revised orbits and (γ, q) = (1, 0), the values obtained for the lumped 31st-order harmonics were:

$$10^{6-0,2}C_{31} = 0.86 \pm 0.32, \qquad 10^{6-0,2}S_{31} = -1.21 \pm 0.20 . \qquad (17)$$

The value of ϵ was 0.56. The fitting of the theoretical curve to the individual values, after removal of perturbations due to atmospheric rotation and lunisolar precession, is shown by the unbroken line in Fig 8. The fit is good, and it is perhaps surprising that the standard deviations of the coefficients are not smaller: this is mainly due to the high correlation between them (0.89). The amplitude of the oscillation in i due to Earth and ocean tides[14] is expected to be about 0.0003° (35 m), and since only one of the 17 values has a standard deviation as low as this, it is not necessary to make any adjustments for the tidal effects.

The orbits were also fitted using (γ, q) = (1, 0), (1, 1) and (1, -1); but ϵ scarcely changed, and the extra coefficients were indeterminate. A further fitting, with (γ, q) = (1, 0) and (2, 0), resulted in a 4% increase in ϵ, little change in the lumped 31st-order harmonics (though their sd increased by more than 75%), and indeterminate values for the 62nd-order terms, which therefore appear to be of no significance.

The standard deviations of the values (17) should be reliable: THROE works on the assumption that the orbits are independent, and this seems fair, because there were only two orbits for which a few observations at the end were re-used at the beginning of the next orbit, to make up the numbers. Errors due to error in the chosen value of Λ are not taken into account, but should not be

significant because a change of 0.1 in λ alters the values of the coefficients by less than 25% of their sd.

6.4 Analysis of eccentricity

The eccentricity of a nearly circular orbit like that of 1973-27B suffers important perturbations from the effects of (a) the odd zonal harmonics in the geopotential and (b) atmospheric drag: both these perturbations need to be carefully removed if the effects of the resonance are to be exposed. Lunisolar perturbations are small and easily removed.

The perturbations produced by the effects of odd zonal harmonics on a drag-free orbit of low eccentricity are well-known[22]; but their removal from an orbit suffering other unknown perturbations (due to drag and resonance) raises many difficulties. The method adopted here was as follows. The variation of eccentricity with time on a drag-free orbit, initially coinciding with that of 1973-27B, was calculated by numerical integration at 1-day intervals with the aid of the PROD computer program[18], for a gravitational field with zonal harmonics up to the 20th, plus lunisolar perturbations. The variation in e, which may be denoted by Δe_{ZH}, gives the perturbation of eccentricity on the drag-free (and resonance-free) orbit due to zonal harmonics and lunisolar perturbations. In the absence of drag, Δe_{ZH} depends* on the argument of perigee ω, and it was assumed here that the appropriate value of Δe_{ZH} to be subtracted from the observed value of e at each epoch was the value given by the drag-free calculation *not* at the epoch, but at the slightly different date when ω on the drag-free orbit had the same value as on the actual orbit. This difference, though never more than 1 day, was significant because the values of ω on the actual orbits differed from those on the drag- and resonance-free orbits by up to 3°, and a 3° change in ω changes Δe_{ZH} by 4×10^{-6}, which is comparable with the standard deviation of some of the values. If the actual values of ω differed more widely from those on the drag-free orbits, this method would be open to criticism, but it seems likely to be accurate enough here.

Fig 9a shows the values of eccentricity from the PROP orbits, e_p, as circles, and the values of e_1 after removal of odd zonal harmonic and

---

* On a drag-free orbit, $\Delta e_{ZH} = e - \left\{e^2 - 2e\beta \sin\omega + \beta^2\right\}^{\frac{1}{2}}$, where e is the observational value of eccentricity, and β is a constant expressible[22] in terms of the odd zonal harmonic coefficients, J_3, J_5 etc. $\left[\beta = \frac{R \sin i}{2aJ_2}\left(-J_3 + \text{terms in } J_5, \text{ etc}\right)\right]$. For 1973-27B, $\beta = 802 \times 10^{-6}$. If e is not too small, β is the amplitude of the oscillation in e caused by odd zonal harmonics.

lunisolar perturbations by the method described above, as triangles. ($e_1 = e_p - \Delta e_{ZH}$). The approximately sinusoidal variation in e, indicated by the broken line, has been removed with apparent success, but there remains a considerable variation in e attributable to air drag and possibly resonance*.

The values of e_1 were now used as input for a THROE run, and (after removal of air drag perturbations within THROE) were fitted by the theoretical equation (9). As in the fitting of inclination, H was given its mean value of 45 km, since the mean value of $z = ae/H$ was near 0.4, and the scale height for use in the theory should be evaluated at a height $0.4H$ above perigee when $z = 0.4$ (see Fig 6.3 of Ref 23). This fitting of e_1 by THROE proved disastrous, giving $\epsilon = 8.8$: it was clear that a fundamental error was being made.

The error was fairly obvious - a failure to allow for the day-to-night variation in air density. At heights near 350 km with low solar activity, the maximum air density (in the afternoon) exceeds the minimum (at night) by a factor of about 3. The air drag model within THROE takes no account of this day to-night variation in air density, which can have a great effect on a near-circular orbit[8]. To illustrate the effect, assume that $e = 0.0035$, so that apogee is 45 km higher than perigee (if $a \approx 6700$ km); with $H = 45$ km, the density at perigee would be 2.8 times greater than the density at apogee, in the absence of day-to-night variation. Suppose first that perigee is at the day-time maximum of density and the apogee at the night-time minimum: then the perigee density would exceed the apogee density by a factor of about 9. In these circumstances the orbit contracts like a normal orbit of higher eccentricity, with e^2 decreasing linearly and proportional to the remaining lifetime of the satellite. Thus, since the remaining lifetime is about 200 days, e^2 would decrease by 10% in 20 days. I suppose the situation is reversed, with perigee at the night-time minimum and apogee at the day-time maximum. Then the air density at apogee is slightly *greater* than at perigee, and drag is likely to be nearly constant round the orbit. In these circumstances e^2 would remain very nearly constant, and might even increase slightly, instead of decreasing by 10% in 20 days.

---

* Odd zonal harmonic perturbations have to be removed outside THROE, because the effects of air drag are treated within THROE by using PROP subroutines in which the values of eccentricity are corrected for air drag on the assumption that they are not seriously perturbed by any force other than air drag. For many orbits, this procedure is of adequate accuracy, but for 1973-27B the change in the perturbation in e between successive orbits can be an appreciable fraction of e itself: for example, between MJD 42309 and 42317, where $10^3 e \approx 2.0$, the perturbation to $10^3 e$ changes by 0.4 (see Fig 9a). In these circumstances the values of e have to be cleared of perturbations before being used in THROE.

A general analytical theory for the effects of the day-to-night variation in air density on orbits with $z > 1$ is available[24]; but when $z < 1$ the results[8] are very complicated, except in certain special cases, *eg* low drag, or constant sun-perigee angle, or weak day-to-night variation. Unfortunately 1973-27B does not qualify for any of the special categories, so an analytical correction for the day-to-night variation in air density is not available, and the correction has to be made to each orbit individually. The correction has been applied using a simplified theory given in the Appendix, which assumes that the atmospheric density depends on the geocentric angular distance from the point M of maximum density, taken to be on the equator at 14h local time (the time indicated by *CIRA 1972*). The geocentric angle ϕ_p between M and perigee for 1973-27B during the resonance phase is shown in Fig 10, with the local time at perigee marked on the curve, and M at either 14h or 16h local time (the time indicated in Jacchia's 1977 model[25]). In calculating the effects between orbit n and orbit (n + 1) the mean value of ϕ_p between the two orbits is taken, and the correction to be applied for the effect of the day-to-night variation, e_{DN}, is found by integrating from orbit to orbit. The values of e_{DN} for the 17 orbits, shown in Fig 9b, are far from negligible: the total change is 0.5×10^{-3}, which may be regarded as equivalent to 3 km in perigee distance; and even the 2-hour change in the time of assumed maximum density has an appreciable effect.

With e_{DN} available, a doubly corrected value of e, given by $e_2 = e_1 + e_{DN}$ can be formed and the values of e_2 can be fitted using THROF. The previous attempt to fit e_1 had been disastrous because the fitting was not only bad but also gave no hint as to how improvements might be made: nearly all the values seemed to be wrong - as in fact they were. When the values of e_2 were fitted with equation (9) by using THROE there was a great reduction in ϵ, from 8.8 to 4.1, and there was also a clear indication that three values (at MJD 42232, 42245 and 42303) were failing to fit. It would have been possible to omit these values, but the numerical integration of $\dot{\Phi}$ would then be over different time-intervals in the fittings of i and of e: it is better to keep the values of Φ exactly the same as on the fittings of i and of e, by adopting the alternative strategy of increasing the standard deviations of the ill-fitting values by an arbitrary factor of 10, to destroy their influence. With this alteration, the value of ϵ decreased from 4.1 to 1.72.

The effect of changing the assumed local time of the maximum density from 14h to 16h was now tested. The value of ϵ increased from 1.72 to 2.95, so it was clear that maximum density at 14h gave much better results.

In the fitting with $\epsilon = 1.72$, there were still two somewhat errant orbits, at MJD 42238 and 42324. At each of these epochs there were several earlier runs (nearly as good as the final orbit), on which the values of e differed by up to 3 sd from the value on the final orbit used to obtain e_2 : the sd of e was therefore increased by a factor of $\sqrt{10}$ on these two orbits. With this change, the value of ϵ fell from 1.72 to 1.08: this fitting still left room for improvement, however, because the largest weighted residual (1.6) was for the orbit at MJD 42245, for which the sd had already been increased by a factor of 10. In least-squares fitting, the largest weighted residual has the greatest effect on the sum of squares, and it would be absurd to allow this 'discarded' orbit to exert so great an influence; so its sd was increased by a further factor of 1.6.

The resulting (and final) fitting of the values of e_2 by THROE, shown by the unbroken line in Fig 11, gave $\epsilon = 1.03$ and yielded determinate values for all four of the lumped harmonics, as follows:

$$10^6 \bar{C}_{31}^{-1,1} = 18.0 \pm 10.0 \qquad 10^6 \bar{S}_{31}^{-1,1} = 26.8 \pm 11.1 \ , \qquad (18)$$

$$10^6 \bar{C}_{31}^{-1,3} = -38.2 \pm 4.2 \qquad 10^6 \bar{S}_{31}^{-1,3} = 19.4 \pm 2.8 \ . \qquad (19)$$

In Fig 11, the weighted residuals for the three values with grossly inflated standard deviations (shown by squares) are 1.1, 1.0 and 0.6: their rms, 0.93, is quite close to the overall rms, 1.03. So these three orbits do not significantly affect either the fitting or the sd of the lumped coefficients. When these three orbits were omitted and the remaining 14 orbits were fitted, the value of ϵ increased from 1.03 to 1.06, and the values of the lumped coefficients changed by less than 10% of their sd in (18) and (19).

The effect of taking the point M of maximum density at 16h local time instead of 14h was tested by making a further THROE run with the values of e_2 suitably altered. The value of ϵ was 1.58, as compared with 1.03 with M at 14h. This comparison is not entirely fair because the accuracies of some orbits were adjusted to improve the fitting when M was at 14h local time. When M is at 16h, the orbit at MJD 42324 no longer requires its sd increasing by a factor of $\sqrt{10}$, but the value at MJD 42238 requires a further relaxation: so the sd of th first was divided by $\sqrt{10}$ and that of the second multiplied by $\sqrt{10}$. A new fitting by THROE, with these changes, give $\epsilon = 1.34$, still considerably higher. Thus the results are sensitive to the assumed local time of maximum density, and a better fit is achieved with M assumed to be at 14h.

6.5 Simultaneous fitting of i and e

The SIMRES computer program[17] allows a simultaneous fitting of i and e for one or more satellites. If the e terms in equation (8) are important, it is clearly preferable to make a simultaneous fitting, with $(\gamma, q) = (1, 0)$, $(1, 1)$ and $(1, -1)$. But for 1973-27B the e terms in equation (8) are not expected to be large, so the advantage of a simultaneous fitting is in doubt and must be judged empirically.

The fitting was made with the weighting of the e values degraded by a factor of 1.58, which is the ratio of the values of e on the fitting of e and i by THROE used as input for SIMRES. The values of the lumped coefficients in the simultaneous fitting were

$$10^6 \bar{C}_{31}^{0,2} = 1.46 \pm 0.39 \qquad 10^6 \bar{S}_{31}^{0,2} = -1.12 \pm 0.25 \ , \qquad (20)$$

$$10^6 \bar{C}_{31}^{1,1} = 20.8 \pm 10.1 \qquad 10^6 \bar{S}_{31}^{1,1} = 24.7 \pm 11.4 \ , \qquad (21)$$

$$10^6 \bar{C}_{31}^{-1,3} = -36.1 \pm 4.3 \qquad 10^6 \bar{S}_{31}^{-1,3} = 17.8 \pm 2.8 \ . \qquad (22)$$

The fittings of i and e using these coefficients are shown by the broken lines in Figs 8 and 11. The SIMRES fitting of i is considerably worse than the fitting of i alone with $(\gamma, q) = (1, 0)$, the sum of squares of weighted residuals in inclination being 6.7 instead of 4.4. With e the simultaneous fitting is almost as good as the fitting of e alone.

6.6 Discussion

It is difficult to decide whether to recommend the values from the individual fittings, equations (17)-(19), or the values from the simultaneous fitting, equations (20)-(22), or a mixture of the two. If the results from i and e were equally reliable, the simultaneous fitting would be preferable. But if i is more reliable than e, the results obtained from fitting i alone could be 'contaminated' by being forced to accept less reliable values of the $(\gamma, q) = (1, \pm 1)$ terms dictated by the variations in e. Noting that (a) the correction e_{DN} to e was very sensitive to the assumed form of the day-to-night variation in air density, (b) three values of e failed to fit, and (c) two others were given increased sd, we have to conclude that the fitting of i is more reliable than that of e. The probable difference in reliability seems

great enough to justify a preference for the fitting of i alone, equations (17). This opinion - and it is only an opinion, not a certainty - is reinforced by the fact that the unbroken curve in Fig 8 fits much better than the broken curve, which is disturbingly oscillatory. For eccentricity, the choice is not important, since the values (18) and (19) are so close to (21) and (22). If i is more reliable, the fitting of e should benefit from a contribution by i and the values from the simultaneous fitting, (21) and (22), are therefore preferred.

Of the three pairs of lumped coefficients, (17), (21) and (22), the third pair may seem the most accurate because of their proportionally smaller sd. But it is probably fairer to compare the absolute values of each sd after division by the largest numerical coefficient in equations (14)-(16) respectively. If equation (14) is written in descending numerical order of coefficients, we have:

$$\left.\begin{aligned} \bar{C}_{40,31} - 0.799\bar{C}_{42,31} - 0.701\bar{C}_{38,31} + \ldots &= 0.0112\bar{C}^{0,2}_{31} \\ &= (9.0 \pm 3.6) \times 10^{-9} \\ \bar{S}_{40,31} - 0.799\bar{S}_{42,31} - 0.701\bar{S}_{38,31} + \ldots &= (-13.6 \pm 2.2) \times 10^{-9} \end{aligned}\right\} \quad (23)$$

on using the value of $\bar{C}^{0,2}_{31}$ from (17). Similarly, for S ,

Equation (15), treated in the same way, yields

$$\left.\begin{aligned} \bar{C}_{41,31} - 0.801\bar{C}_{43,31} - 0.707\bar{C}_{39,31} + \ldots &= (-21 \pm 10) \times 10^{-9} \\ \bar{S}_{41,31} - 0.801\bar{S}_{43,31} - 0.707\bar{S}_{39,31} + \ldots &= (-25 \pm 12) \times 10^{-9} \end{aligned}\right\} \quad (24)$$

Equation (16), with similar rearrangement, gives

$$\left.\begin{aligned} \bar{C}_{39,31} - 0.893\bar{C}_{41,31} - 0.617\bar{C}_{37,31} + \ldots &= (134 \pm 16) \times 10^{-9} \\ \bar{S}_{39,31} - 0.893\bar{S}_{41,31} - 0.617\bar{S}_{37,31} + \ldots &= (66 \pm 10) \times 10^{-9} \end{aligned}\right\} \quad (25)$$

Looked at in this light, the first pair of coefficients emerges as the most accurate.

The geopotential coefficients of degree ℓ are expected to be of order of magnitude $10^{-5}/\ell^2$, that is, of order 6×10^{-9} for $\ell \sim 40$. So the lumped coefficients, being made up of perhaps 10 or 15 significant terms, might be expected to be of magnitude 20×10^{-9}. The pairs (23) and (24) fulfil this expectation; but the pair (25) does not, and the $\bar{C}$ coefficient in particular seems unduly large. No explanation of this anomaly can be offered at present.

The values of the lumped 31st-order coefficients depend critically on inclination and the numerical factors in the expressions (14)-(16) look quite different to those in the corresponding expressions[2] for Proton 4 (inclination 51.5°, as opposed to 50.0°). For example, $\bar{C}_{41,31}$ is multiplied by - 979.6 in (15) and by - 534 for Proton 4; $\bar{C}_{43,31}$ is multiplied by 784.4 in (15) and by 256 for Proton 4. The equation from Proton 4 corresponding to the anomalous C equation in (25) is

$$\bar{C}_{39,31} - 0.585\bar{C}_{41,31} - 0.743\bar{C}_{37,31} + \ldots = (61 \pm 18) \times 10^{-9} \quad .$$

So Proton 4 also gives a large and positive value, on the right-hand side, though the numerical factors on the left-hand side differ enough to rule out any strict comparison.

7 UPPER-ATMOSPHERE ROTATION

7.1 Perturbations in inclination

The values of inclination, after removal of relevant perturbations, should show a continual decrease produced by the effects of upper-atmosphere rotation, and it is possible to determine the upper-atmosphere rotation rate Λ from the variation in inclination. Fig 6 shows the values of inclination after removal of zonal harmonic, $J_{2,2}$, and lunisolar perturbations, as described in section 6.3, with the curve of Fig 8 drawn in across the resonance region.

In assessing the significance of other perturbations, it should be remembered (a) that only one of the 62 orbits has a nominal accuracy better than 30 m, and (b) that the satellite was 25 m long, and that the observations relied on reflections, either radar or optical, coming from any part of it. Because of these uncertainties, perturbations of order 50 m or less must be regarded as negligible. Among these negligible perturbations are the effects of Earth and ocean tides (35 m), solar radiation pressure (10 m) and meridional winds (20 m). The unimportance of meridional winds may seem surprising, because such winds can have appreciable effects on an eccentric orbit when the perigee is at particular local times. Meridional winds have a diurnal variation, however, being away from

the equator by day and towards the equator by night[26], and for a nearly circular orbit like that of 1973-27B, they will tend to cancel. Even if the meridional winds are consistently in one direction, however, their effects still tend to cancel on a near-circular orbit. The effect of a constant 100 m/s south-to-north wind on the orbit of 1973-27B has been calculated: the maximum change in inclination produced was 0.00016° (19 m), which must be regarded as an upper limit, since a constant wind is unrealistic.

Theoretical curves of the variation of inclination with time for 1973-27B have been calculated for a range of atmospheric rotation rates Λ using the program ROTATM, which is based on a lengthy theoretical equation (quoted explicitly by Walker[10]), which takes account of atmospheric oblateness, and the variation of scale height with height. The only other effect which might be influential is that of the day-to-night variation in density, but theory[27] indicates that this effect is small unless the orbit is close to certain conditions of resonance between the motion of the Sun and that of the perigee: these conditions do not arise for 1973-27B.

7.2 Rotation rate from June 1973 to July 1974

Between launch and the 31:2 resonance, the theoretical curve with $\Lambda = 1.04$ best fits the points in Fig 6. The fit is entirely satisfactory, and the value of Λ is quite accurately determined by the end points. The first 8 orbits serve to define the starting value as $50.0442^{\circ} \pm 0.0002^{\circ}$. The final value can be specified in two ways: either (a) from the group of three accurate independent values near MJD 42200, which gave $50.0390^{\circ} \pm 0.0002^{\circ}$ at MJD 42210, equivalent to $50.0385^{\circ} \pm 0.0002^{\circ}$ at MJD 42232; or (b) by the curve of Fig 8, which shows that the mean of the oscillatory fitted curve is 0.0006° above the observational value of MJD 42232, giving $50.0387^{\circ} \pm 0.0002^{\circ}$ (on doubling the nominal sd). Both (a) and (b) therefore give essentially the same result and if we assume that $i = 50.0386^{\circ} \pm 0.0002^{\circ}$ at MJD 42232, the decrease in inclination from the start is $0.0056^{\circ} \pm 0.00028^{\circ}$, giving an error of $\pm 5\%$ in Λ. Thus $\Lambda = 1.04 \pm 0.05$ between 17 June 1973 and 4 July 1974. This value is averaged over local time, because (a) the orbit is so nearly circular and (b) the (ill-defined) perigee moves through two day-to-night cycles between MJD 41850 and 42232 (see Fig 15).

To find the effective height y_{Λ} at which this first value of Λ applies, we note that the mean perigee height between June 1973 and July 1974 (see Fig 16) was 355 km, where, from *CIRA 1972*, the average value of H in 1973-4 was 50 km. The average value of $z = ae/H$ is therefore 0.7 and theory[20] indicates that y_{Λ}

should be taken at 0.5H above perigee. So Λ applies at a mean height of 380 km, with a possible error of about 5 km.

The curve drawn through the mean values of Λ obtained in previous analyses[21,28], reproduced in Fig 12, shows a maximum of about 1.3 at a height of 350 km with a rapid decrease to about 1.0 at a height of 400 km. The value obtained from 1973-27B, namely 1.04 ± 0.05 at 380 ± 5 km, is below the curve, and suggests that the decrease in Λ may occur at a height about 20 km lower than the curve suggests - at least in 1973-1974.

For 1973-27B, the effective height y_Λ decreases from 390 km initially to 365 km in July 1974: so, if the curve of Fig 12 is correct, the value of Λ should increase between June 1973 and July 1974. A slightly lower value over the first six months and a slightly higher value over the next six months, would fit the values in Fig 6 just as well; but the decrease in inclination is too small to justify more than a single mean value.

7.3 The 31:2 resonance (4 July to 10 October 1974)

In the analysis of the resonant variation of inclination (section 6.3), better results were obtained with $\Lambda = 1.3$ than with $\Lambda = 1.2$. This cannot be called an 'evaluation' of Λ, but does show that the observed variations are consistent with a value of Λ of 1.3. The effective height y_Λ is 350 km, and the value is shown by a diamond in Fig 12.

7.4 Rotation rate from 10 October 1974 to decay (11 January 1975)

The value of inclination at the end of resonance is of course just as well defined as that at the beginning, and from Fig 8 it appears that the last value in the resonance period, at MJD 42330 (10 October 1974), coincides with the mean of the oscillatory fitted curve. So this value of inclination, namely 50.0371° (after removal of $J_{2,2}$, lunisolar and zonal harmonic perturbations), serves as a secure starting point for the continuation of the theoretical curve. The nominal accuracy of the value, 0.0001°, can appropriately be doubled to allow for other sources of error, such as the averaging of Earth and ocean tide perturbations.

The most accurate value of inclination between MJD 42330 and decay is that at MJD 42393, namely 50.0294° (after removal of perturbations). It seems appropriate to select Λ so that the theoretical curve passes close to this point: if we take $\Lambda = 1.34$, all the observational values between MJD 42330 and MJD 42409 are satisfied to within 1.1 sd. Fig 13 shows the observational values and the

theoretical curve for $\Lambda = 1.34$ with a time scale wider than in Fig 6. Some of the values beyond MJD 42409 are also satisfied by the $\Lambda = 1.34$ curve, but the last four values are far above this curve, and it is obvious that a lower value of Λ is required at the end of the life. The value which best satisfies the last four points is $\Lambda = 1.06$, and this curve intersects the $\Lambda = 1.34$ curve at a date close to MJD 42409 (1974 Dec 28). So the theoretical curves chosen to fit the values are $\Lambda = 1.34$ for MJD 42330-42409 and $\Lambda = 1.06$ for MJD 42409-42423. The change-over or 'hinge-point' at MJD 42409 is marked with a black disc in Fig 13. (Using more than two values of Λ would give a closer fit, but the two-value fitting is adequate because it satisfies all the points to within 1.1 sd.)

The accuracy of these two determinations of Λ is quite difficult to assess. It seems reasonable to assume that the curve is accurate to 0.0005° at MJD 42393, where the observational value has sd 0.0005° and several other points nearby are adequately fitted. But the two further points, at MJD 42402 and 42409, do not strengthen the accuracy: they merely confirm it. So the $\Lambda = 1.34$ curve will be taken as applying between MJD 42330 and 42393, and as measuring a decrease of 0.0080° in inclination with an accuracy of 0.00054° (or adding in the error of 0.0002° at the start). This gives $\Lambda = 1.34 \pm 0.09$. Between MJD 42330 and 42393 the perigee height decreases almost linearly from 316 km to 266 km, with a mean of 290 km (see Fig 16); so the effective height y_{Λ} is 305 ± 5 km, being 0.4H above perigee, where $H = 40$ km.

The $\Lambda = 1.06$ curve at the end of the life fits the last four points very well, and since their mean sd is 0.0006°, the curve should be accurate to about 0.0003° at the end of the life. In assigning an error to the starting value, at MJD 42409, we note that if the $\Lambda = 1.34$ curve is accurate to 0.0005° at MJD 42393, the extra error incurred through Λ being 10% in error thereafter would be 0.0004°, giving a root-square total of 0.0006° at MJD 42409. If we accept this assessment, the error in Λ is 6%, or 0.06. It could be argued that the task of assigning a realistic error is impossible, but a tentative estimate is still helpful. The height at which the value $\Lambda = 1.06$ applies is also questionable: the mean of the first and last perigee heights is 200 km, but the curve is largely determined by the last four values, when the perigee height decreases from 201 to 157 km, with a mean of 180 km. It seems reasonable to take the mean perigee height as 190 ± 10 km. An addition of 0.3H, where $H = 30$ km, gives $y_{\Lambda} = 200 \pm 10$ km.

7.5 Analysis in terms of orbital period

When $e < 0.006$ and $z < 0.8$, as for 1973-27B, the lengthy theoretical equation[10] giving the change Δi in inclination when the orbital period T_d changes by ΔT_d may be simplified to

$$\frac{\Delta i}{\Delta T_d} = \frac{\Lambda \sin i}{6\sqrt{F}} \left\{ 1 + \frac{I_2(z)}{I_0(z)} (1 + c) \cos 2\omega + \tfrac{1}{3}c + O(0.01) \right\} , \qquad (26)$$

where $I_n(z)$ is the Bessel function of the first kind and imaginary argument, of degree n and argument z; the factor $\sqrt{F}$ is nearly equal to 1, being given by $\sqrt{F} \approx 1 - 0.040\Lambda$ for 1973-27B; and c expresses the effect of atmospheric oblateness, with $c \sim 0.15$ for 1973-27B. Since $I_2/I_0 < 0.07$ for $z < 0.8$, the variation of i with T_d should be nearly linear if Λ is constant; thus, when the variation of i with time is non-linear, as with 1973-27B after resonance, a clearer picture emerges if i is plotted against T_d, as in Fig 14. After resonance, $z < 0.4$, so that $I_2/I_0 < 0.02$, and the oversimplification of assuming that constant Λ corresponds to constant slope is correct to ±2%. The unbroken lines in Fig 14 correspond to the $\Lambda = 1.34$ and $\Lambda = 1.06$ curves in Fig 13, and both have been continued as broken lines beyond the hinge-point at MJD 42409, marked by the black disc. The need for two slopes is obvious, and although the exact choice of slope and of the hinge-point is arguable, there is apparently no other preferable pair of hinged lines passing through the point at the end of resonance.

7.6 Discussion

The three values of atmospheric rotation rate (rev/day) obtained from this analysis of 1973-27B are:

$\Lambda = 1.04 \pm 0.05$ at height 380 ± 5 km, for June 1973 to July 1974;

$\Lambda = 1.34 \pm 0.09$ at height 305 ± 5 km, for 10 October to 28 Dec 1974;

$\Lambda = 1.06 \pm 0.06$ at height 200 ± 10 km, for 28 Dec 1974 to 11 Jan 1975.

All three values are averaged over local time, because the orbit is so nearly circular. (For the third value the local time at perigee is near midnight, as Fig 15 shows; but the orbit is very nearly circular, with $e \sim 0.001$, and the midnight perigee would tend to equalize the drag round the orbit.)

The values of Λ obtained here are not especially accurate, because the total decrease in inclination is quite small (0.03°); but the values do have the virtue that they cover a wide range of height. The existing curve for the variation of Λ with height, reproduced in Fig 12 - showing Λ near 1.0 at 200 km, 1.3 at 350 km and 1.0 at 400 km - is based on a compilation of results from many different satellites, at different dates, latitudes, etc. Now this curve has for the first time been tested by results from a single satellite, with confirmation of its general form, though the decrease in Λ at heights between 350 and 400 km may have occurred at a lower height in 1973-4.

Average values of Λ lower than those given by the curve of Fig 12 have been obtained in two recent papers[10,11] for heights of 220-320 km during the years 1971-1975. These results, from analysis of the satellites 1971-106A (inclination 66°) and 1971-18B (inclination 70°), are in conflict with the high value of Λ (1.34) obtained from 1973-27B at 305 km during the last three months of 1974. The difference may be a latitude effect, resulting from the lower inclination of 1973-27B: a tendency for low-inclination satellites to give high values of Λ has been noted previously[21], and it is probable that most of the 'super-rotation' of the upper atmosphere occurs at latitudes below 45°.

7.7 Comments on the accuracy of the orbital model in PROP

There is one further question which arises when (as here) the values of inclination obtained are pressed to the limits of their formal accuracy to extract information on Λ. The question may be posed provocatively in the form: "Is the sd of a PROP orbit at a particular epoch invalidated by the neglect of lunisolar perturbations within the PROP model during the 5 days or so over which the observations extend?"

Lunisolar perturbations for 1973-27B have been computed at daily intervals using PROD[18]. For eccentricity, the results show that lunisolar perturbations are negligible, never more than 2 m: this is because e itself is so small. For inclination, the variations are much larger, often of order 50 m over five days. The orbits likely to be affected are the most accurate ones, namely orbits Nos. 2, 8, 14, 15, 19, 23, 27 and 34, for which the sd in inclination is less than 50 m. The *maximum* departures of i from its value at epoch, due to lunisolar perturbations during the days covered by the observations for these nine orbits are 28 m, 89 m, 3[illegible] m, 24 m, 43 m, 45 m, 36 m, 19 m and 38 m respectively. Since (a) the epoch is always taken as near as possible to the mid-point in time of the observations, and (b) the perturbation in i is usually monotonic over five days (if not, it is small), the orbit determined will tend to average out the

perturbations not included in the PROP model, so that the resultant error in inclination at epoch, δ_{LS} say, should not be more than about $\frac{1}{4}$ of the maximum perturbation, as recorded above. For eight of the nine orbits, the value of δ_{LS}, thus defined, is less than $\frac{1}{3}$ of the standard deviation σ of the inclination as given in Table 1, and therefore would not be expected to affect σ appreciably.

The one doubtful orbit is No.8, the most accurate of all, which unfortunately also has the largest lunisolar perturbation. For this orbit PROP gives $\sigma = 0.00012^{\circ}$, which is equivalent to 14m, and the lunisolar perturbations in i at 00 hours on the 7 days centred on epoch (expressed as equivalent distances) are: 89 m, 66 m, 35 m, 0, -33 m, -55 m, -66 m. The variation with time is nearly linear, except for the last value, so the averaging effect implicit in the orbit determination should ensure that errors from this source do not much exceed 10 m. The accuracy can also be assessed from a different argument: it is the Hewitt camera observations that are responsible for σ being as small as 14 m, and there were two sets of these camera observations, at 2 hours and at 27 hours after epoch. Since these observations are dominant, the orbit will be 'most correct' about 14 hours after epoch, with the lunisolar perturbations well away from epoch easily falling within the observational accuracy of the less accurate observations available there. (The nominal accuracy of the observations is 5 m for the Hewitt camera, and 200 m or more for the other observations.) This argument indicates the importance of taking the epoch for orbit determination as close as possible to the Hewitt camera observations. In the 14h between epoch and the time when orbit No.8 is 'most correct' the lunisolar perturbation is 19 m: to be realistic, therefore, the standard deviation of i on orbit 8 probably needs to be doubled, to 0.0002°. No change in the analysis is required, since 0.0002° has already been taken as the accuracy for the mean of the first eight orbits. Nor is any change needed in Fig 6, where even a doubled sd is still too small to show.

8 ANALYSIS OF VARIATIONS IN ECCENTRICITY DUE TO AIR DRAG

8.1 Decrease in $a(1 - e)$

If the variations in eccentricity due to zonal harmonic and lunisolar perturbations are removed, the remaining variation in e (outside the resonance region) should be caused almost entirely by the effect of atmospheric drag. If we accept the theory for the effect of air drag[24], the variation in e can be analysed to determine either (a) values of scale height H, if the factor F

defining the amplitude of the day-to-night density variation* is assumed known, or (b) values of F, if H is assumed known. Alternatively, we can assume that the values of H and F given by *CIRA 1972* are correct - because previous orbit analyses[10,11] indicate that the *CIRA* values of H are correct to ±10% for 1973-4 - and then compare the variation of eccentricity predicted by theory with the observed variation. The latter approach has been adopted here, because the theory for an atmosphere with day-to-night variation in density has not previously been tested. We work with $a(1 - e)$ rather than e because the zonal harmonic perturbation can be more accurately removed (the third harmonic perturbation to e, Δe_{J3}, is given by $J_3 R \sin i \sin \omega / J_2 a$, so that $a\Delta e_{J3}$ remains of constant amplitude as the orbit contracts).

The values of $a(1 - e)$ from the 62 orbits, plotted as triangles in Fig 15, have an oscillation caused chiefly by the effect of odd zonal harmonics in the geopotential. The values of $a(1 - e)$ have been cleared of zonal harmonic and lunisolar perturbations using the computer program PROD with integration at 1-day intervals. The orbits given by PROD are drag-free, and the integration was restarted whenever ω on the drag-free orbit departed from the real value by more than 3°. As explained in section 6.4, the perturbation removed from $a(1 - e)$ was the value indicated by PROD at the correct value of ω rather than at the correct epoch.

The values of $a(1 - e)$ cleared of these perturbations are denoted by Q and plotted as circles in Fig 15. It will be seen that Q continually decreases: as expected, its slope is generally least when the local time at perigee is near 14h (when the density is near maximum) and greatest when the local time at perigee is near 04h.

Theory[24] indicates that the decrease of the eccentricity (cleared of gravitational perturbations) should be governed by the equation

$$\frac{da}{dx} = \frac{I_0(z) + I_1(z) F \cos \phi_p}{I_1(z) + \frac{1}{2}\{I_0(z) + I_2(z)\} F \cos \phi_p} \{1 + 0(e)\} , \qquad (27)$$

where ϕ_p is the geocentric angular distance between the perigee and the point M of maximum density (as in section 6.4), $z = x/H$, and x is the value of a cleared of perturbations, so that $x = a - Q$, whence $dQ/da = 1 - dx/da$. Thus the theory gives

* The definition of F (see equation (A-1) of the Appendix) is such that the ratio of maximum to minimum density is $(1 + F)/(1 - F)$. For 1973-27B during most of its life, $F \sim 0.5$, so that the ratio is about 3.

$$\frac{dQ}{da} = 1 - \frac{I_1 + \frac{1}{2}(I_0 + I_2)F \cos \phi_p}{I_0 + I_1 F \cos \phi_p} \{1 + 0(0.005)\} , \qquad (28)$$

on dropping the argument z. If values of H and F for the appropriate values of height, solar activity, etc, are taken from *CIRA 1972*, the right-hand side of equation (28) gives theoretical values of dQ/da, which can be compared with the observed values of $\Delta Q/\Delta a$ on orbits taken far enough apart to ensure that the change ΔQ in Q between the two orbits can be accurately determined. Although the average sd in $a(1 - e)$ is 80 m, the correction for zonal harmonic and lunisolar perturbations may introduce errors of a similar order because of the discrepancies between the values of ω on the drag-free and actual orbits. Thus, when two values of Q are differenced to obtain ΔQ, an error of about 0.2 km can be expected, and if an accuracy better than 5% in $\Delta Q/\Delta a$ is required, values of ΔQ of 4 km or more should be used.

The histogram in Fig 17 shows the observational values of $\Delta Q/\Delta a$, calculated on this basis. (The first value of ΔQ is only 2.6 km, but it should still be accurate to ±5%, being based on an average over 9 orbits.) Fig 17 also shows the values of dQ/da given by the right-hand side of equation (28) when values of H and F are taken from *CIRA 1972* at the appropriate satellite perigee height, as given by Fig 16, and the appropriate exospheric temperature, taken constant at 800K (because there was little variation in solar activity in 1973-4). The shape of the curve joining the calculated values of dQ/da is drawn to correspond with the rather erratic variation of ϕ_p, shown at the top of Fig 17. The broken curve in Fig 17 shows the values of dQ/da given by theory with no day-to-night variation in density ($F = 0$).

Comparison of the theoretical and observational values of dQ/da in Fig 17 shows excellent agreement, usually well within the possible ±5% error in the observational values. The resonance region ought to be excluded from the comparison, because other perturbations occur; but even here the agreement is quite good, except on the first value of $\Delta Q/\Delta a$ (which is affected by the large increase in e between MJD 42232 and 42251 visible in Fig 11).

The theoretical curve with $F = 0$, shown by the broken line in Fig 17, provides a good average value; but the theory with day-to-night variation in density is obviously much better. Its departure from the mean curve is approximately proportional to F, so (if we accept the theory) we can ask whether F is too small or too large. The answer seems to be that F is approximately correct, thus confirming again the general accuracy of *CIRA 1972*.

The values of dQ/da in Fig 17 before resonance are on average about 2% lower than the observational values of $\Delta Q/\Delta a$: this bias could be corrected by an increase of about 4% in the assumed value of H. Although the observational values have a 5% sd, the bias of 2% does persist over six successive values of $\Delta Q/\Delta a$, so it is probably significant. If so, the conclusion is *either* that the *CIRA* values of H are about 4% too low *or* that H should be evaluated at a height γH above perigee (where $\gamma \sim 0.5$ here). The latter seems more likely to be the correct conclusion and it fits in with the simplified theory of the Appendix, where H has to be evaluated at the mean of the perigee and apogee heights. This would imply that the treatment of H in an atmosphere where H varies with height[23] can be carried over into the theory for an atmosphere with day-to-night density variation. This latter theory has so far only been developed[24] on the assumption of constant H.

8.2 Variation of perigee height

The distance of perigee from the Earth's centre is $\{a(1 - e) + dr_p\}$, where dr_p is a small perturbation[29] which may be written

$$dr_p = \frac{1.726R}{a(1-e)}\left[\sin^2 i - e(3 - \tfrac{7}{2}\sin^2 i) + e^2(4 - 5\sin^2 i) - 2(1 - e + e^2)\sin^2 i \sin^2\omega + 0(e^3)\right] \quad \text{km} . \tag{29}$$

For 1973-27B, with error less than 30 m,

$$dr_p = 0.97 - 1.94 \sin^2\omega \quad \text{km} . \tag{30}$$

The perigee height y_p is obtained by subtracting the local Earth radius $R_p (= 6378.14 - 21.38 \sin^2 i \sin^2\omega)$ from the perigee distance. Thus, for 1973-27B,

$$y_p = a(1 - e) - (6371.86 + 5.31 \cos 2\omega) . \tag{31}$$

The values of y_p are plotted in Fig 16, which has already been used in choosing values of H and in assessing the effective height y_Λ at which Λ applies. The high peaks in Fig 16 occur when perigee is at maximum latitude south; the lower peaks at northern apex.

8.3 Values of eccentricity near decay

The values of eccentricity in Fig 3, after tracing out a spiral locus through most of the satellite's life, shift to a different path during the last

8 days, because (a) the decrease in e due to drag begins to overcome the increase due to odd zonal harmonics, and (b) the day-to-night variation in air density begins to have an increasing influence on the argument of perigee.

The general equations for the variation of the eccentricity of a near-circular orbit in an atmosphere with day-to-night variation in density[8] involve lengthy expressions with Fresnel integrals of three different arguments. The equations simplify, however, as decay approaches and indicate that $z \to |F \cos \phi_p|$ and $\omega \to \tan^{-1}(-\cos i \tan M')$, where $M' = \Omega - L - 30^\circ$, if the maximum of the daytime bulge is at 14h local time and on the equator. Here L is the solar longitude, which increased from 282° on 3 January 1975 to 290° on 11 January 1975 (the day of decay). The theoretical equations also indicate that $\cos \phi_p \to -(\cos^2 i + \sin^2 i \cos^2 M')^{\frac{1}{2}}$ at decay.

This theory has not been subjected to a practical test, because no high-drag circular orbit has been determined with sufficient accuracy at daily intervals. It is therefore useful to test the theory by trying to interpret the variations of e and ω for 1973-27B in its last days. The limiting values quoted in the previous paragraph may be regarded as 'end-values' towards which the orbit would be moving in the absence of the odd zonal harmonic perturbations. Let the suffix F denote these 'final' values, so that, on any of the last days of the satellite's life, we can obtain values of z_F, ω_F and ϕ_{pF} from the equations

$$z_F = |F \cos \phi_p| \tag{32}$$

$$\omega_F = \tan^{-1}(-\cos i \tan M') \tag{33}$$

$$\cos \phi_{pF} = -(\cos^2 i + \sin^2 i \cos^2 M')^{\frac{1}{2}} \quad . \tag{34}$$

Values of z_F and ω_F have been calculated for each of the last 7 orbits and are plotted as triangles linked by a broken line in Fig 18, in the $(z \cos \omega, z \sin \omega)$ plane.

The corresponding observational values of $z \cos \omega$ and $z \sin \omega$ from the last 7 orbits (with one exception) are indicated by circles in Fig 18. The exception is 7 January, for which the values of e and ω in Table I give a non-conforming point, indicated by a cross; this point could be omitted, but instead it has been replaced by values of e and ω from a previous orbit at the same epoch, for which $10^3 e = 1.248$ and $\omega = 31.5^\circ$. These are the values indicated by the circle in Fig 18. (This orbit is also used in Fig 3, with the orbit of Table I as a cross.)

In the absence of air drag, the future variation of z and ω in Fig 18 would be (approximately) motion round a circle centred at the point $\left(0, \frac{0.8a}{10^3 H}\right)$. This point is the equivalent of the point C in Fig 3, but it is no longer fixed because H decreases steadily, from 32 km on 3 January to 19 km on 11 January. The single-headed arrows in Fig 18 show the expected progress along the appropriate circle in one day (or 3 days for the first point) on the basis of a 6° daily advance. Drag has the effect of 'attracting' the point away from this path and towards the relevant triangle: this 'attraction' is suggested by double-headed arrows, their length being (arbitrarily) increased as decay approaches.

At first, drag has little effect and the actual path is close to the circle; but drag gradually takes command, and by January 11.0 the drag and gravitational effects are in opposite directions, with the drag dominant. As height decreases, F (and hence z_p) tends to zero and so both loci in Fig 18 are heading towards the origin.

Thus the actual variations of z and ω are as would be expected on the basis of the theory.

The theory also predicts that a nearly circular orbit decaying in an atmosphere with a day-to-night variation in density will adjust its perigee position so that the perigee moves towards the point of minimum density in the orbital plane. When perigee is at the minimum-density point, ϕ_p always exceeds 90° but cannot reach 180° unless the orbital plane happens to pass through the minimum-density point.

In Fig 19 the triangles show the values of ϕ_{pF} in the last days of the satellite's life, from equation (34), which assumes that the point of maximum (or minimum) density is on the equator. The circles in Fig 19 show values of ϕ_p on the actual orbits.

Fig 19 provides strong support for the theory, since the real values of ϕ_p are not only $\geq 90^\circ$, as expected, but also within 15° of the corresponding ϕ_{pF}. In early January the point of minimum density is likely not to be on the equator, as assumed, but at a latitude perhaps[25] as high as 30°N; the effect of such a change may be roughly assessed by taking a smaller value of inclination in equation (34). If i is taken as 35° instead of 50°, the curve of ϕ_{pF} in Fig 19 moves upward and nearly coincides with ϕ_p, as shown by the dotted line. So even the small difference between ϕ_p and ϕ_{pF} in Fig 19 can be explained.

9 CONCLUSIONS

9.1 Orbit determination

An average accuracy of about 90 m radially and across-track was achieved in 62 orbit determinations, based on the observations listed in Table 2. Accurate daily orbits were determined in the six days before decay, with the aid of NORAD and US Navy observations.

There was unacceptable scatter among the values of inclination originally obtained. This scatter, which was eventually eliminated, resulted partly from the slight overweighting of geographically isolated observations, and partly from the inherent defects of least-squares fitting.

9.2 The 31:2 resonance

The variations in inclination and eccentricity during 31:2 resonance (July-October 1974) were successfully analysed, after some difficulties over the removal of perturbations in eccentricity caused by the day-to-night variation in density. The analysis yielded values of six lumped geopotential harmonics of order 31. In these lumped coefficients, harmonics of degree up to 60 are significant and the lumped values should provide a test of the accuracy of coefficients of order 31 and degree 31 to 60 in future evaluations of the geopotential which go to order and degree 60 or more. (Current models[30] do not go beyond order and degree 36.)

9.3 Atmospheric rotation

Three good values of the average atmospheric rotation rate have been obtained over a wide range of height. These show, for the first time from a single satellite, the peak in the rotation rate at heights of 300-350 km. Going upwards in height, the values are 1.06 ± 0.06 rev/day at 200 ± 10 km in January 1975, 1.34 ± 0.09 rev/day at 305 ± 5 km for October-December 1974, and 1.04 ± 0.05 at 380 ± 5 km for June 1973-July 1974.

9.4 Variations in eccentricity

During most of its life the satellite was moving through an atmosphere with a large day-to-night variation in density, which strongly influences the orbital eccentricity: the day-time maximum density exceeded the night-time minimum by a factor of about 3, and the ellipticity of the orbit was nearly equal to the ellipticity of this day-to-night 'bulge'. The variation in $a(1 - e)$ was predicted using theory[24] previously untested and values of atmospheric parameters

from *CIRA 1972*: the predicted values agreed well with the observed variations in $a(1 - e)$ due to drag, thus vindicating both the theory and *CIRA 1972*.

The daily orbits near decay were accurate enough to provide a practical test of the specialized (and also untested) theory[8] for near-circular orbits about to decay in an atmosphere with day-to-night variation in density. The theory gives specific end-values for e and ω and predicts that perigee should, in defiance of the normal effects of the J_2 harmonic, move towards the point of minimum density on the orbit. Both these predictions were tested and satisfactorily confirmed.

Appendix

CORRECTION TO ECCENTRICITY TO REMOVE THE EFFECT OF THE DAY-TO-NIGHT VARIATION IN AIR DENSITY

Quite realistic models now exist which specify the variation of upper-atmosphere density with height, local time and latitude. Here we require the best simple approximation, and we assume (as in Ref 24) that the air density ρ at a fixed height y depends only on the angular distance ϕ from the point M of maximum day-time density, taken to be on the equator at 14h local time, and is given by

$$\rho(y) = \bar{\rho}(y)\{1 + F \cos \phi\} \quad , \tag{A-1}$$

where $\bar{\rho}$ is the mean density (when $\phi = 90^{\circ}$) and F is a constant, which has a value near 0.5 in the atmosphere sampled by 1973-27B. When $\phi = 90^{\circ}$ (mean day-to-night conditions), we assume that the variation of density with height can be approximated by an exponential,

$$\bar{\rho}(y) = \bar{\rho}_p \exp\left(-\frac{y - y_p}{\bar{H}}\right) \quad , \tag{A-2}$$

where $\bar{\rho}_p$ is the mean density at the perigee height y_p, and $\bar{H}$ is a mean density scale height - the value which gives the best fit to the actual density at heights between perigee and apogee, that is, for $y_p \leq y \leq y_p + 2ae$. In practice, of course, the variation of ρ with ϕ is not exactly symmetrical, as in equation (A-1), and the variation of $\bar{\rho}$ with height is not exactly exponential.

On combining equations (A-1) and (A-2), we have

$$\rho(y) = \bar{\rho}_p\{1 + F \cos \phi\} \exp\left(-\frac{y - y_p}{\bar{H}}\right) \quad , \tag{A-3}$$

for heights between perigee and apogee. Evaluating (A-3) first at apogee and then at perigee, and dividing, we have

$$\frac{\rho_a}{\rho_p} = \frac{1 + F \cos \phi_a}{1 + F \cos \phi_p} \exp\left(-\frac{2ae}{\bar{H}}\right) \quad , \tag{A-4}$$

where ρ_a, ρ_p are the densities at apogee and perigee respectively, and ϕ_a, ϕ_p the corresponding values of ϕ. In calculating the changes in e due to air drag, the theory[23] calls for a value of $\bar{H}$ appropriate to a height

044

$y_p + \gamma H$, where γ is a function of $z = ae/H$. For orbits with $z > 2$, $\gamma = 1.5$; but for 1973-27B at 31:2 resonance, z is near 0.4, for which $\gamma \simeq 0.4$ (Fig 6.3 of Ref 23). Thus, for 1973-27B, H should be evaluated at a height $y_p + 0.4H$, which happens to be half-way between perigee and apogee height, since $0.4H \simeq ae$. This means that H may be taken equal to $\bar{H}$, which has already been defined as the appropriate mean value of density scale height between perigee and apogee. Thus $z = ae/\bar{H}$ and since $\phi_a = \phi_p + 180^\circ$, equation (A-4) becomes

$$\frac{\rho_a}{\rho_p} = \frac{1 - F \cos \phi_p}{1 + F \cos \phi_p} \exp(-2z) \quad . \tag{A-5}$$

Over a time interval of a few days, when ϕ_p can be regarded as fixed, the simplest way of approximating to an atmosphere with a day-to-night density variation is to define an 'effective scale height' H_E and a corresponding $z_E = ae/H_E$, such that a simple exponential model with scale height H_E will give the same result as (A-5). Thus we require

$$\frac{\rho_a}{\rho_p} = \exp(-2z_E) \tag{A-6}$$

or, on using (A-5),

$$z_E = z + \tfrac{1}{2} \ln \frac{1 + F \cos \phi_p}{1 - F \cos \phi_p} \quad . \tag{A-7}$$

So the appropriate value of z_E at each epoch can be evaluated if F and ϕ_p are known.

If the orbit is symmetrical relative to the 'day-time bulge' of density, *ie* if $\phi_p = 0$ or 180° , the variation of density round the orbit should be well approximated by a spherically symmetrical atmosphere with scale height H_E . In asymmetrical situations the approximation is not so good, but fortunately the effects of high drag on one side of perigee and low drag on the other (at the same numerical value of eccentric anomaly E) combine to produce the same effect as their mean, because $\dot{e}$ depends only on $\cos E$ and not on $\sin E$ (see Ref 23, equation 4.11). So the use of H_E , though obviously inexact, is a basically stable approximation.

For 1973-27B in July-October 1974, the mean perigee height was near 330 km, and, guessing $\bar{H} = 50$ km , we have to evaluate H at a height $0.4\bar{H} = 20$ km

above perigee, that is at 350 km. The mean level of solar 10.7 cm radiation was 90×10^{-22} W m^{-2} Hz^{-1}, so with an allowance of 40 K for geomagnetic disturbance, the mean day/night exospheric temperature for use in the COSPAR International Reference Atmosphere 1972 is 800 K, from *CIRA 1972*, page 265. The *CIRA* tables then give $\bar{H} = 45$ km for $y = 350$ km, and also show that the ratio of maximum day-time to minimum night-time density is 2.8, giving $F = 0.47$. Thus $a/\bar{H} = 150$ and $z = ae/\bar{H} = 150e$. Hence values of z_E can be obtained from equation (A-7) for each of the 17 orbits in the resonance region, taking $F = 0.47$ and values of ϕ_p from Fig 10.

Within THROE, the air-drag correction to e between orbit n at epoch t_n and orbit $(n + 1)$ at epoch t_{n+1}, is taken as

$$\Delta e_T = \frac{4\bar{M}_2}{3M_1} y_1(z) \cdot (t_{n+1} - t_n) , \qquad (A-8)$$

where $\bar{M}_2$ is defined in section 6.1, M_1 is the value at epoch t_n, and $y_1(z)$ is a ratio of Bessel functions, approximated by[31]

$$y_1(z) = \frac{240z + 153z^2 + 68z^3 + 24z^4}{480 + 306z + 196z^2 + 80z^3 + 24z^4} . \qquad (A-9)$$

Equation (A-8) assumes a spherically symmetrical atmosphere: to allow for the effect of the day-to-night variation we need to replace z by z_E in (A-8). Thus, since THROE already makes the correction Δe_T, the *extra* correction required to take account of the day-to-night variation is Δe_{DN}, given by

$$\Delta e_{DN} = \left\{ \frac{y_1(z_E)}{y_1(z)} - 1 \right\} \Delta e_T . \qquad (A-10)$$

The total correction at the nth epoch, e_{DN}, is found by summing the values of Δe_{DN} between epochs 1 and 2, epochs 2 and 3, ..., epochs $(n - 1)$ and n. The values of Δe_T for use in (A-10) were derived initially from a previous THROE run and improved by iteration, only one iteration being needed. The values of e_{DN} are shown in Fig 9b, the full line giving the values when M is taken at 14h local time, as indicated by *CIRA 1972*, and the broken line when M is taken at 16h local time, as indicated in Jacchia's 1977 atmospheric model[25]. Changing M to 16h significantly changes e_{DN} and considerably worsens the fit of the

theoretical curve to the values of e (see section 6.4). Thus the simple model used here works better if M is taken at 14h. According to the recent MSIS atmospheric model[32], the local time for maximum density varies during the course of the year between 14h and 16h.

Table 1

VALUES OF THE ORBITAL PARAMETERS AT THE 62 EPOCHS, WITH STANDARD DEVIATIONS

	MJD	Date	a	e	i	Ω	ω	ω + M_0	M_1	M_2	M_3	M_4	M_5	a(1 − e)	c	N	D
1	41850.0	1973 Jun 17	6777.003	0.006011	50.0455	215.085	37.9	5.548	5601.606	0.0426	–	–	–	6736.27	0 68	50	5.9
			<1	20	11	3	2		1	3				13			
2	*41855.0	1973 Jun 22	6776.622	0.006175	50.0432	189.214	57.1	316.119	5602.078	0.0408	–	–	–	6734.78	0.42	48	4.0
			1	11	3	2	1		1	3				7			
3	*41861.0	1973 Jun 28	6776.114	0.006298	50.0418	158.158	79.5	116.046	5602.707	0.0573	–	–	–	6733.44	0.87	72	5.6
			1	12	7	2	2		1	3				8			
4	*41866.0	1973 Jul 3	6775.656	0.006306	50.0459	132.279	98.0	72.433	5603.276	0.0439	–	–	–	6732.93	0.62	43	4.9
			1	9	11	2	2		1	6				6			
5	41874.0	1973 Jul 11	6775.156	0.006132	50.0476	90.858	128.4	295.348	5603.897	0.0387	−0.0006	–	–	6733.61	0.61	55	7.0
			1	13	7	1	1		1	2	1			9			
6	41881.0	1973 Jul 18	6774.726	0.005735	50.0460	54.604	155.6	314.420	5604.430	0.0356	–	–	–	6735.87	0.76	47	5.3
			<1	24	10	2	1		1	4				16			
7	41889.0	1973 Jul 26	6774.231	0.005173	50.0440	13.163	188.9	186.430	5605.044	0.0497	0.0016	–	–	6739.19	0.58	40	6.3
			1	10	9	1	1		1	3	2			7			
8	*41908.0	1973 Aug 14	6772.898	0.004491	50.0459	274.687	281.7	221.166	5606.699	0.0286	–	–	–	6742.48	0.55	68	8.1
			<1	4	1	<1	1		<1	1				3			
9	*41919.0	1973 Aug 25	6772.241	0.004829	50.0429	217.650	335.3	25.696	5607.514	0.0665	0.0015	–	–	6739.54	0.40	52	5.5
			1	15	5	1	1		1	2	2			10			
10	*41926.0	1973 Sep 1	6771.420	0.005169	50.0455	181.340	6.0	71.823	5608.534	0.0732	–	–	–	6736.42	0.75	74	7.9
			<1	9	7	2	1		<1	2				6			
11	41946.0	1973 Sep 21	6769.014	0.005864	50.0419	77.502	83.5	40.282	5611.524	0.0772	0.0031	–	–	6729.32	0.42	35	7.2
			1	8	10	1	1		1	2	1			5			
12	41966.0	1973 Oct 11	6765.972	0.005090	50.0468	333.517	158.2	77.204	5615.309	0.0591	–	–	–	6731.53	0.69	44	6.3
			1	10	12	2	1		1	3				7			
13	41981.0	1973 Oct 26	6764.433	0.004163	50.0438	255.438	223.7	144.676	5617.225	0.0745	–	–	–	6736.27	0.53	58	4.3
			1	16	11	2	3		1	6				11			
14	*41986.0	1973 Oct 31	6763.661	0.003952	50.0447	229.392	249.6	174.453	5618.186	0.1028	−0.0061	–	–	6736.93	0.52	53	5.1
			1	12	3	2	3		1	2	3			8			
15	*41992.0	1973 Nov 6	6762.965	0.003897	50.0458	198.134	279.0	72.211	5619.054	0.0599	−0.0014	–	–	6736.61	0.60	98	6.9
			1	6	4	1	2		1	2	1			4			
16	42013.0	1973 Nov 27	6761.122	0.004898	50.0444	88.649	18.6	104.130	5621.351	0.0734	−0.0023	–	–	6728.01	0.49	49	7.3
			<1	5	8	1	1		1	1	1			3			
17	42021.0	1973 Dec 5	6760.351	0.005288	50.0458	46.915	50.0	113.363	5622.314	0.0593	–	–	–	6724.60	0.69	50	6.3
			1	8	9	1	1		1	3				5			
18	42045.0	1973 Dec 29	6758.369	0.005145	50.0446	281.614	139.4	180.123	5624.785	0.0548	0.0007	–	–	6723.60	0.61	50	5.8
			1	8	9	2	1		1	2	1			5			
19	*42077.0	1974 Jan 30	6755.471	0.003690	50.0444	114.342	289.7	3.931	5628.405	0.0474	−0.0008	–	–	6730.54	0.68	68	8.3
			<1	8	3	1	1		<1	1	1			5			
20	42100.0	1974 Feb 22	6753.230	0.004798	50.0444	353.956	35.4	344.816	5631.207	0.0876	0.0014	–	–	6720.82	0.50	55	6.9
			1	6	6	1	1		1	2	1			4			
21	42120.0	1974 Mar 14	6750.258	0.004917	50.0396	249.126	109.6	50.411	5634.925	0.1175	0.0005	–	–	6717.07	0.72	37	7.5
			1	9	9	1	1		1	2	1			6			
22	42141.0	1974 Apr 4	6746.430	0.003679	50.0414	138.847	191.0	88.843	5639.722	0.1031	0.0024	–	–	6721.61	0.78	50	7.3
			1	6	9	1	1		1	2	1			4			
23	*42154.0	1974 Apr 17	6744.280	0.003028	50.0406	70.471	254.9	39.363	5642.418	0.1130	0.0068	0.00036	−0.00015	6723.86	0.62	78	8.9
			1	10	3	2	3		1	3	3	2	1	7			
24	42181.0	1974 May 14	6738.964	0.004047	50.0396	288.216	25.1	308.831	5649.096	0.1313	0.0020	–	–	6711.69	0.75	38	7.3
			1	13	14	2	1		1	3	1			9			
25	*42199.0	1974 Jun 1	6735.951	0.004502	50.0399	193.147	92.2	227.443	5652.886	0.1371	0.0018	−0.0010	–	6705.63	0.57	40	6.9
			1	8	5	1	2		1	7	1	1		5			
26	*42204.0	1974 Jun 6	6734.939	0.004417	50.0373	166.723	110.4	76.968	5654.160	0.0936	−0.0174	0.0175	−0.00373	6705.19	0.51	52	4.0
			1	6	3	1	<1		1	11	12	10	23	4			
27	*42210.0	1974 Jun 12	6733.346	0.004200	50.0381	134.985	131.7	191.920	5655.536	0.1461	−0.0021	−0.0009	0.00010	6705.56	0.59	70	8.5
			1	14	3	1	1		1	5	2	1	1	9			

Table I (continued)

	MJD	Date	a	e	i	Ω	ω	ω + M_0	M_1	M_2	M_3	M_4	M_5	a(1 − e)	c	N	D
28	42232.0	1974 Jul 4	6730.346 1	0.002817 13	50.0393 12	18.484 2	229.4 3	199.381	5659.948 1	0.1248 15	0.0145 6	–	–	6711.39 9	0.48	27	4.2
29	42238.0	1974 Jul 10	6728.814 1	0.002694 9	50.0387 11	346.668 2	263.7 1	351.516	5661.860 1	0.1205 1	-0.0030 1	–	–	6710.69 6	0.63	39	7.9
30	42245.0	1974 Jul 17	6727.718 <1	0.002709 10	50.0414 8	309.529 1	303.5 3	60.413	5663.264 1	0.0945 5	–	–	–	6709.49 7	0.41	29	4.0
31	42251.0	1974 Jul 23	6726.840 1	0.003147 12	50.0419 16	277.674 2	336.4 2	229.499	5664.372 2	0.1344 4	0.0088 2	–	–	6705.67 8	0.70	37	6.4
32	42255.0	1974 Jul 27	6725.939 1	0.003313 9	50.0401 11	256.432 2	355.0 2	226.971	5665.511 1	0.1185 9	–	–	–	6703.66 6	0.47	27	3.4
33	42259.0	1974 Jul 31	6725.164 <1	0.003487 17	50.0372 10	235.176 1	12.3 2	228.551	5666.490 1	0.1203 3	–	–	–	6701.71 11	0.56	37	5.6
34	*42264.0	1974 Aug 5	6723.993 1	0.003713 22	50.0369 3	208.592 1	33.1 2	146.308	5667.970 1	0.1643 6	-0.0092 4	–	–	6699.03 13	0.44	34	3.8
35	*42268.0	1974 Aug 9	6723.060 1	0.003862 14	50.0384 4	187.313 1	48.7 2	158.102	5669.150 1	0.1529 5	-0.0007 1	–	–	6697.10 9	0.61	41	6.0
36	42275.0	1974 Aug 16	6721.488 1	0.004028 12	50.0414 11	150.052	73.7 3	280.090	5671.139 1	0.1376 3	0.0009 2	–	–	6694.41 8	0.50	32	5.7
37	42283.0	1974 Aug 24	6719.216 1	0.003966 8	50.0408 9	107.428 1	101.5 1	335.336	5674.015 1	0.1683 2	-0.0036 1	–	–	6692.57 5	0.40	26	7.2
38	42289.0	1974 Aug 30	6717.760 1	0.003743 18	50.0380 13	75.431 2	122.2 3	211.362	5675.860 1	0.1644 5	–	–	–	6692.62 12	0.62	26	4.9
39	42296.0	1974 Sep 6	6715.772 <1	0.003289 8	50.0395 10	38.062 1	148.0 1	21.811	5678.379 <1	0.1904 3	–	–	–	6693.68 5	0.44	29	5.3
40	42303.0	1974 Sep 13	6713.706 1	0.002824 20	50.0418 12	0.658 2	176.2 2	210.538	5681.001 1	0.2091 3	0.0062 2	–	–	6694.75 13	0.47	27	5.5
41	42309.0	1974 Sep 19	6711.164 2	0.002237 10	50.0429 11	328.558 2	203.6 3	132.631	5684.229 2	0.2477 12	0.0076 6	-0.0016 2	–	6696.15 7	0.74	43	5.9
42	42317.0	1974 Sep 27	6708.334 1	0.001745 11	50.0379 13	285.698 2	247.9 6	296.928	5687.826 2	0.2402 16	0.0022 4	-0.0017 2	–	6696.63 7	0.46	23	5.2
43	42324.0	1974 Oct 4	6705.525 1	0.001670 15	50.0374 15	248.136 2	293.4 8	194.633	5691.399 1	0.2943 8	–	–	–	6694.33 10	0.46	20	4.3
44	*42330.0	1974 Oct 10	6702.163 1	0.001719 26	50.0386 5	215.894 2	326.9 5	181.310	5695.681 2	0.4894 13	-0.0132 5	–	–	6690.64 17	0.72	42	4.1
45	42337.0	1974 Oct 17	6696.536 1	0.002081 28	50.0388 13	178.183 2	1.2 4	146.556	5702.862 1	0.4717 3	-0.0135 1	–	–	6682.60 19	0.70	37	7.3
46	42346.0	1974 Oct 26	6691.520 1	0.002440 23	50.0340 18	129.572 2	37.2 4	62.679	5709.274 1	0.3740 7	–	–	–	6675.19 15	0.69	26	5.2
47	42352.0	1974 Nov 1	6687.881 1	0.002684 15	50.0319 16	97.080 2	53.7 3	159.042	5713.934 2	0.4018 5	0.0044 3	–	–	6669.93 10	0.65	30	5.4
48	42359.0	1974 Nov 8	6682.840 3	0.002757 23	50.0350 19	59.089 3	73.4 5	249.618	5720.399 4	0.5138 17	0.0197 11	–	–	6664.42 15	0.76	22	4.3
49	42366.0	1974 Nov 15	6676.689 2	0.002745 13	50.0370 20	21.002 3	93.8 2	31.704	5728.305 3	0.4799 9	-0.0221 8	–	–	6658.36 9	0.88	26	4.6
50	42373.0	1974 Nov 22	6671.425 2	0.002535 16	50.0339 15	342.793 2	116.5 5	223.739	5735.086 2	0.5871 6	0.0068 5	–	–	6654.51 11	0.60	23	5.0
51	42380.0	1974 Nov 29	6664.629 1	0.002219 15	50.0331 15	304.458 2	138.2 4	111.530	5743.859 2	0.5976 8	-0.0068 4	–	–	6649.84 10	0.45	28	4.9
52	*42386.0	1974 Dec 5	6658.594 3	0.001831 12	50.0336 12	271.489 2	161.1 4	64.236	5751.669 4	0.6083 19	-0.0352 27	0.0057 8	–	6646.40 8	0.58	24	3.9
53	*42393.0	1974 Dec 12	6651.417 1	0.001344 21	50.0325 5	232.902 2	192.5 4	67.646	5760.979 1	0.7628 4	-0.0037 2	–	–	6642.48 14	0.59	38	6.0
54	42402.0	1974 Dec 21	6639.195 3	0.000748 21	50.0243 25	183.030 3	258.6 2.3	181.774	5776.891 4	1.205 2	0.0100 14	–	–	6634.23 14	0.58	20	4.0

Table 1 (concluded)

	MJD	Date	a	e	i	Ω	ω	ω + M_0	M_1	M_2	M_3	M_4	M_5	a(1 − e)	ε	N	D
55	42409.0	1974 Dec 28	6624.616 2	0.000942 21	50.0233 13	143.967 2	330.1 9	36.154	5795.969 3	1.626 3	0.0228 12	−0.0071 8	–	6618.38 14	0.68	21	4.0
56	42415.0	1975 Jan 3	6608.475 2	0.001235 17	50.0251 11	110.205 2	5.5 5	341.424	5817.215 3	1.883 5	0.0325 24	0.0483 18	0.0127 7	6600.31 11	0.65	55	4.3
57	42418.0	1975 Jan 6	6596.144 1	0.001245 6	50.0237 8	93.208 1	29.3 5	189.030	5833.533 2	3.451 16	–	–	–	6587.93 4	0.32	46	0.7
58	42419.0	1975 Jan 7	6590.643 3	0.001315 11	50.0229 10	87.510 1	35.3 6	270.777	5840.837 4	4.769 20	–	–	–	6581.98 7	0.71	74	0.8
59	42420.0	1975 Jan 8	6582.937 3	0.001238 5	50.0233 5	81.797 1	35.0 3	1.449	5851.094 4	5.333 7	0.821 28	–	–	6574.79 3	0.43	81	0.9
60	42421.0	1975 Jan 9	6573.295 4	0.001166 6	50.0224 7	76.055 1	39.3 3	103.431	5863.971 5	7.204 11	0.472 39	–	–	6565.63 4	0.57	90	0.8
61	42422.0	1975 Jan 10	6560.104 3	0.001050 7	50.0207 5	70.279 1	44.0 3	220.247	5881.665 4	12.001 8	2.998 25	–	–	6553.22 5	0.50	88	0.9
62	42423.0	1975 Jan 11	6531.434 10	0.000595 7	50.0162 8	64.438 1	55.3 9	2.683	5920.430 14	38.511 56	34.43 36	24.81 71	–	6527.55 5	0.72	87	0.7

* Orbits using Hewitt camera observations

MJD = modified Julian day
a = semi major axis (km)
e = eccentricity
i = inclination (deg)
Ω = right ascension of ascending node (deg)
ω = argument of perigee (deg)
M_0 = mean anomaly at epoch (deg)
M_1 = mean motion n (deg/day)
M_2, M_3, M_4, M_5 = later coefficients in polynomial for M, equation (1)
ε = measure of fit, see section 3.1
N = number of observations used
D = time covered by the observations (days)

The value of a is calculated from n within PROP assuming a gravitational constant $\mu = 398602\ km^3/s^2$.

REFERENCES

No.	Author	Title, etc
1	-	*Skylab news reference*, page I-38. NASA Office of Public Affairs, Washington (1973)
2	H. Hiller D.G. King-Hele	The orbit of Proton 4 redetermined, with geophysical implications. *Planet. Space Sci.*, 25, 511-520 (1977) RAE Technical Report 76143 (1976)
3	R.H. Gooding R.J. Tayler	A PROP 3 user's manual. RAE Technical Report 68299 (1968)
4	R.H. Gooding	The evolution of the PROP 6 orbit determination program, and related topics. RAE Technical Report 74164 (1974)
5	D.M.C. Walker	Variations in air density from January 1972 to April 1975 at heights near 200 km. *Planet. Space Sci.*, 26, 291-309 (1978) RAE Technical Report 77078 (1977)
6	C.J. Brookes P. Moore	Air density at heights near 435 km from the orbit of Skylab 1. *Planet. Space Sci.*, 26, 913-924 (1978)
7	-	*CIRA 1972* (COSPAR International Reference Atmosphere 1972). Akademie-Verlag, Berlin (1972)
8	G.E. Cook D.G. King-Hele	The contraction of satellite orbits under the influence of air drag, Part VI: Near-circular orbits with day-to-night variation in air density. *Proc. Roy. Soc. Lond. A* 303, 17-35 (1968)
9	D.W. Scott	ORES: a computer program for the analysis of residuals from PROP. RAE Technical Report 69163 (1969)
10	D.M.C. Walker	Cosmos 462 (1971-106A): orbit determination and analysis. RAE Technical Report 78089 (1978)
11	H. Hiller	Determination and geophysical interpretation of the orbit of China 2 rocket (1971-18B). RAE Technical Report 78107 (1978)

REFERENCES (continued)

No.	Author	Title, etc
12	C.J. Brookes D. Holland	Analysis of the orbit of 1968-90A (Cosmos 248). *Planet. Space Sci.*, 26, 611-618 (1978)
13	D.G. King-Hele D.M.C. Walker	Analysis of the orbit of 1965-11D (Cosmos 54 rocket). *Planet. Space Sci.*, 21, 1081-1108 (1973) RAE Technical Report 72204 (1972)
14	T.L. Felsentreger J.G. Marsh R.W. Agreen	Analyses of the solid Earth and ocean tidal perturbations on the orbits of the Geos 1 and Geos 2 satellites. *J. Geophys. Res.*, 81, 2557-2563 (1976)
15	W.M. Kaula	*Theory of satellite geodesy.* Blaisdell; Waltham, Mass. (1966)
16	R.R. Allan	Resonance effect on inclination for close satellites. RAE Technical Report 71245 (1971) (Also *Planet. Space Sci.*, 21, 205-225 (1973))
17	R.H. Gooding	Studies of resonance in the orbits of Ariel satellites. RAE Technical Report (to be issued)
18	G.E. Cook	PROD, a computer program for predicting the development of drag-free satellite orbits. Part 1 : theory. RAE Technical Report 71007 (1971) (*Celestial Mechanics*, 7, 301-314 (1973))
19	R.H. Gooding	Lumped geopotential coefficients $\bar{C}_{15,15}$ and $\bar{S}_{15,15}$ obtained from resonant variation in the orbit of Ariel 3. RAE Technical Report 71068 (1971)
20	D.G. King-Hele D.W. Scott	The effect of atmospheric rotation on a satellite orbit, when scale height varies with height. *Planet. Space Sci.*, 17, 217-232 (1969) RAE Technical Report 68066 (1968)
21	D.G. King-Hele D.M.C. Walker	Upper-atmosphere zonal winds: variation with height and local time. *Planet. Space Sci.*, 25, 313-336 (1977) RAE Technical Report 76055 (1976)

REFERENCES (continued)

No.	Author	Title, etc
22	G.E. Cook	Perturbations of near-circular orbits by the Earth's gravitational potential. *Planet. Space Sci.*, 14, 433-444 (1966) RAE Technical Report 65252 (1965)
23	D.G. King-Hele	*Theory of satellite orbits in an atmosphere.* Butterworths, London (1964)
24	G.E. Cook D.G. King-Hele	The contraction of satellite orbits under the influence of air drag, Part V : With day-to-night variation in air density. *Phil. Trans. Roy Soc.* A, 259, 33-67 (1965) RAE Technical Report 64029 (1964)
25	L.G. Jacchia	Thermospheric temperature, density and composition: new models. Smithsonian Astrophysical Observatory Special Report 375 (1977)
26	B.K. Ching J.M. Straus	Ionospheric model effects on thermospheric calculations. *J. Atmos. Terr. Phys.*, 39, 1389-1394 (1977)
27	D.G. King-Hele D.M.C. Walker	The change in satellite orbital inclination caused by a rotating atmosphere with day-to-night variation. *Celestial Mechanics*, 5, 41-54 (1972) RAE Technical Report 70208 (1970)
28	D.M.C. Walker	Upper-atmosphere winds from the orbit of 1973-101A. *J. Brit. Interplan. Soc.*, 31, 197-199 (1978) RAE Technical Memorandum Space 254 (1977)
29	Y. Kozai	The motion of a close Earth satellite. *Astronom. J.*, 64, 367-377 (1959)
30	F.J. Lerch C.A. Wagner S.M. Klosko R.P. Belott R.E. Laubscher W.A. Taylor	Gravity model improvement using Geos 3 altimetry (GEM 10A and 10B). Paper presented at Spring Annual Meeting of the American Geophysical Union, Miami Beach, Florida (1978)
31	R.H. Gooding	A PREP users' manual. RAE Technical Report 69104 (1969)

REFERENCES (concluded)

No.	Author	Title, etc
32	A.E. Hedin J.E. Salah J.V. Evans C.A. Reber G.P. Newton N.W. Spencer D.C. Kayser A. Alcaydé P. Bauer L. Cogger J.P. McClure	A global thermospheric model based on Mass Spectrometer and Incoherent Scatter data, MSIS. 1. N_2 density and temperature. *J. Geophys. Res.*, 82, 2139-2147 (1977)

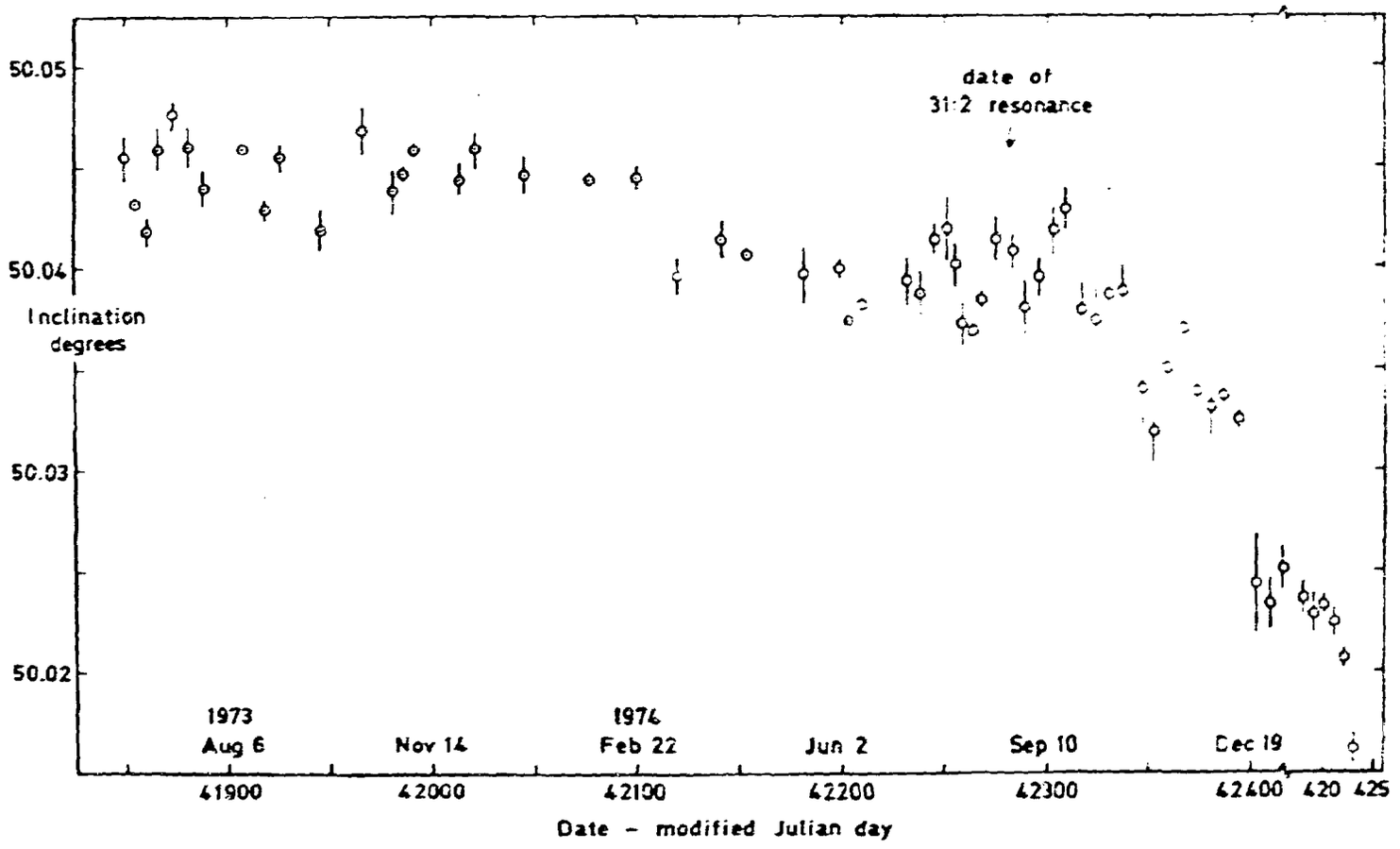

Fig 1 Values of inclination on the 62 orbits

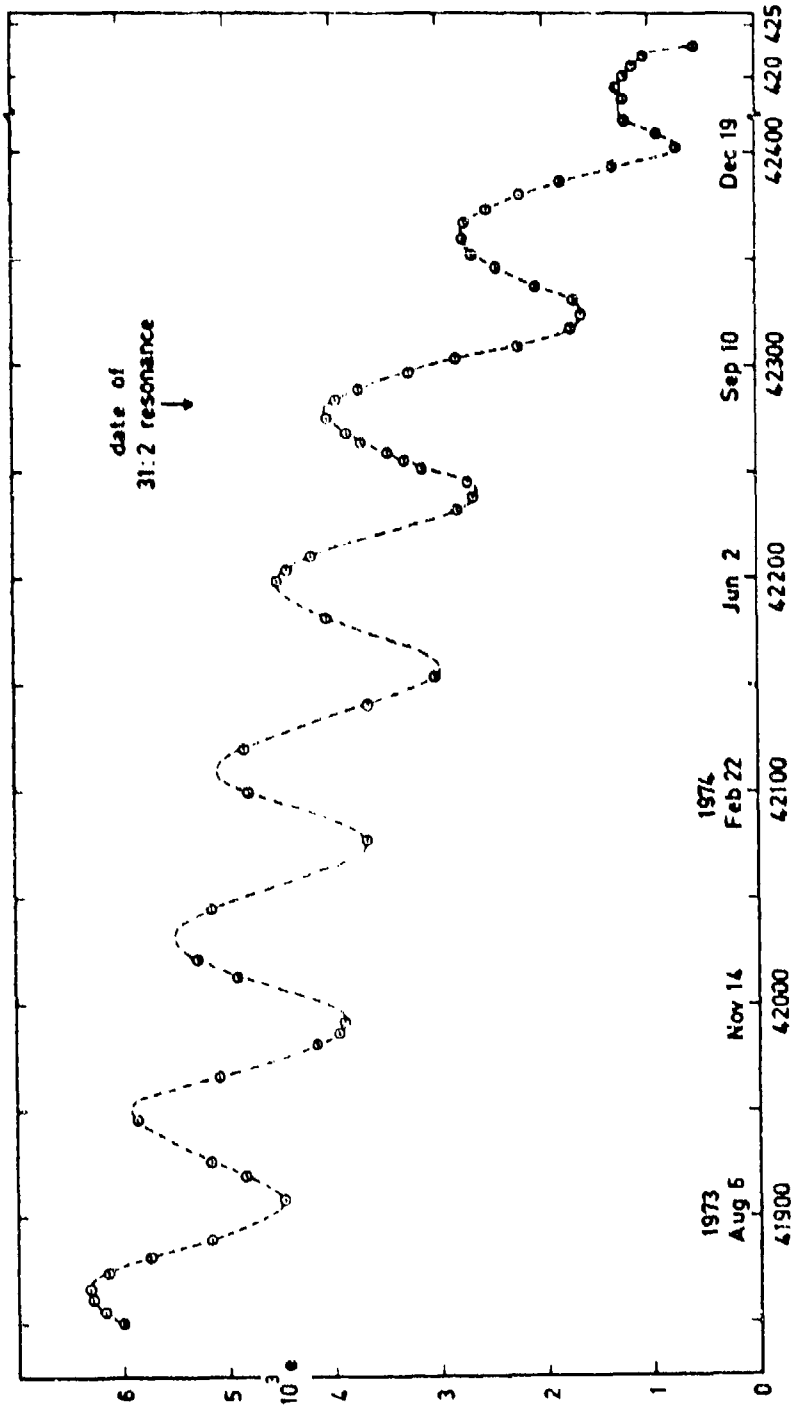

Fig 2 Values of eccentricity on the 62 orbits

Fig 3

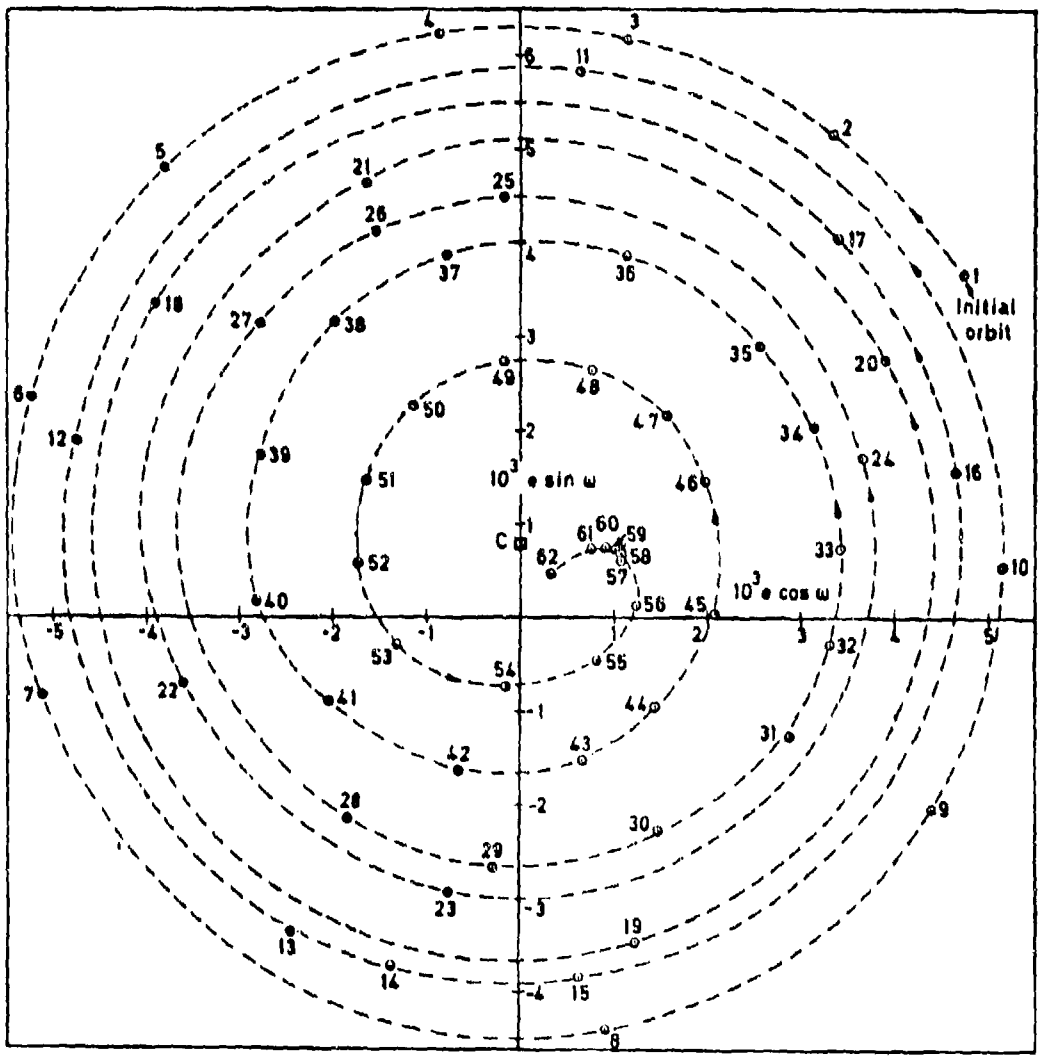

Fig 3 Values of $e \cos \omega$ and $e \sin \omega$ on the 62 orbits

TR 79044

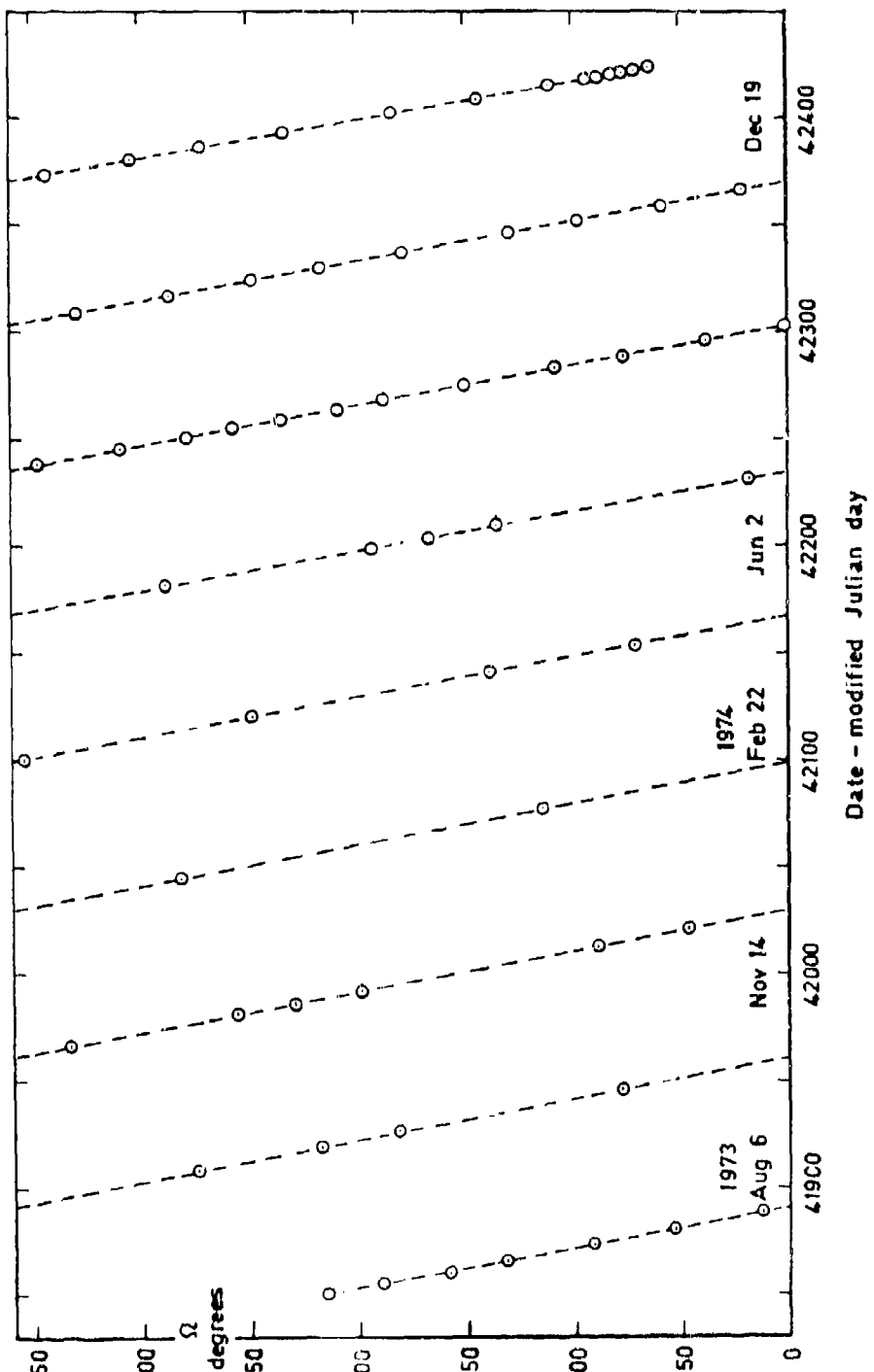

Fig 4 Values of right ascension of node, Ω, on the 62 orbits

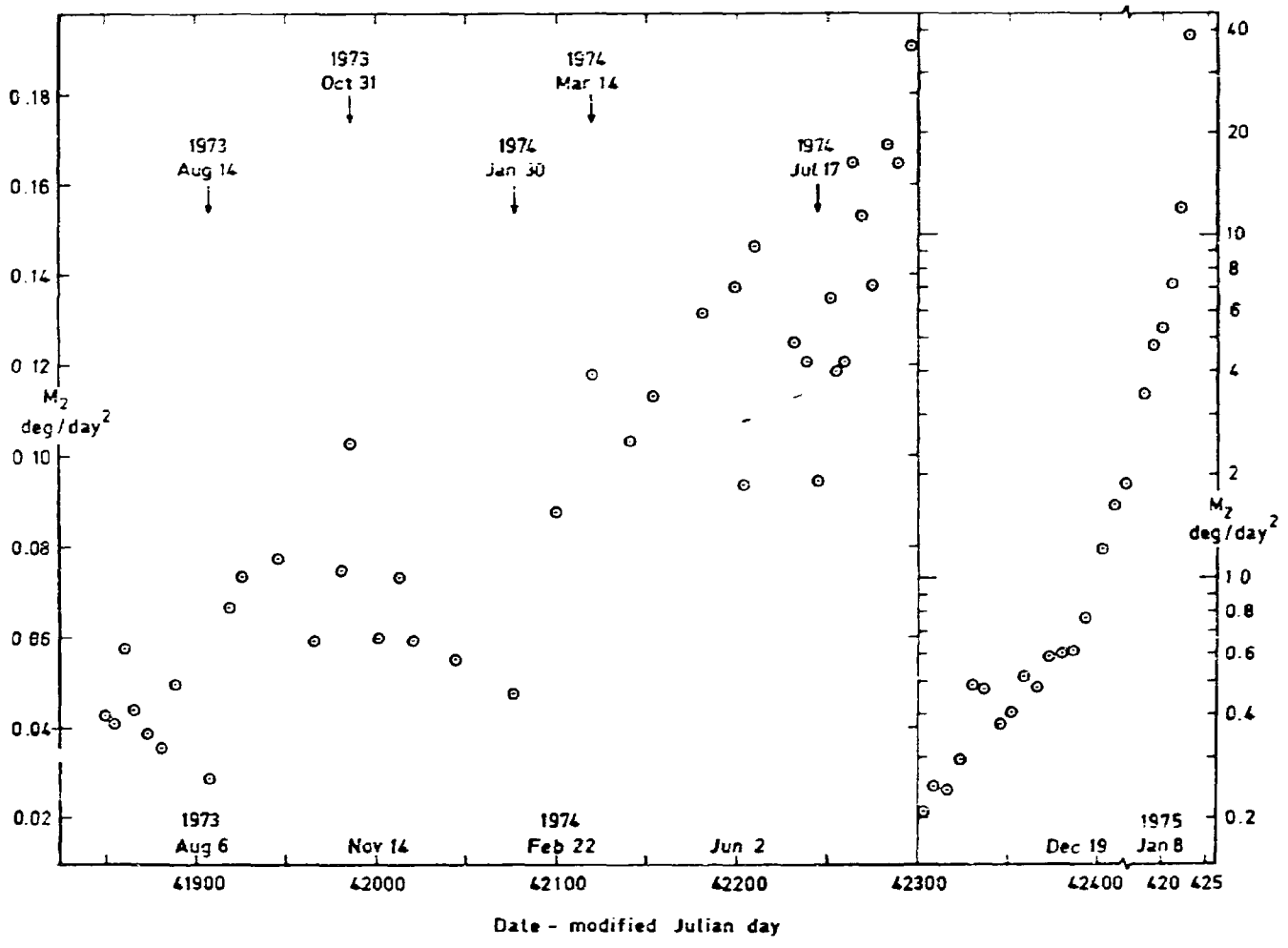

Fig 5 Values of orbital decay rate M_2 on the 62 orbits

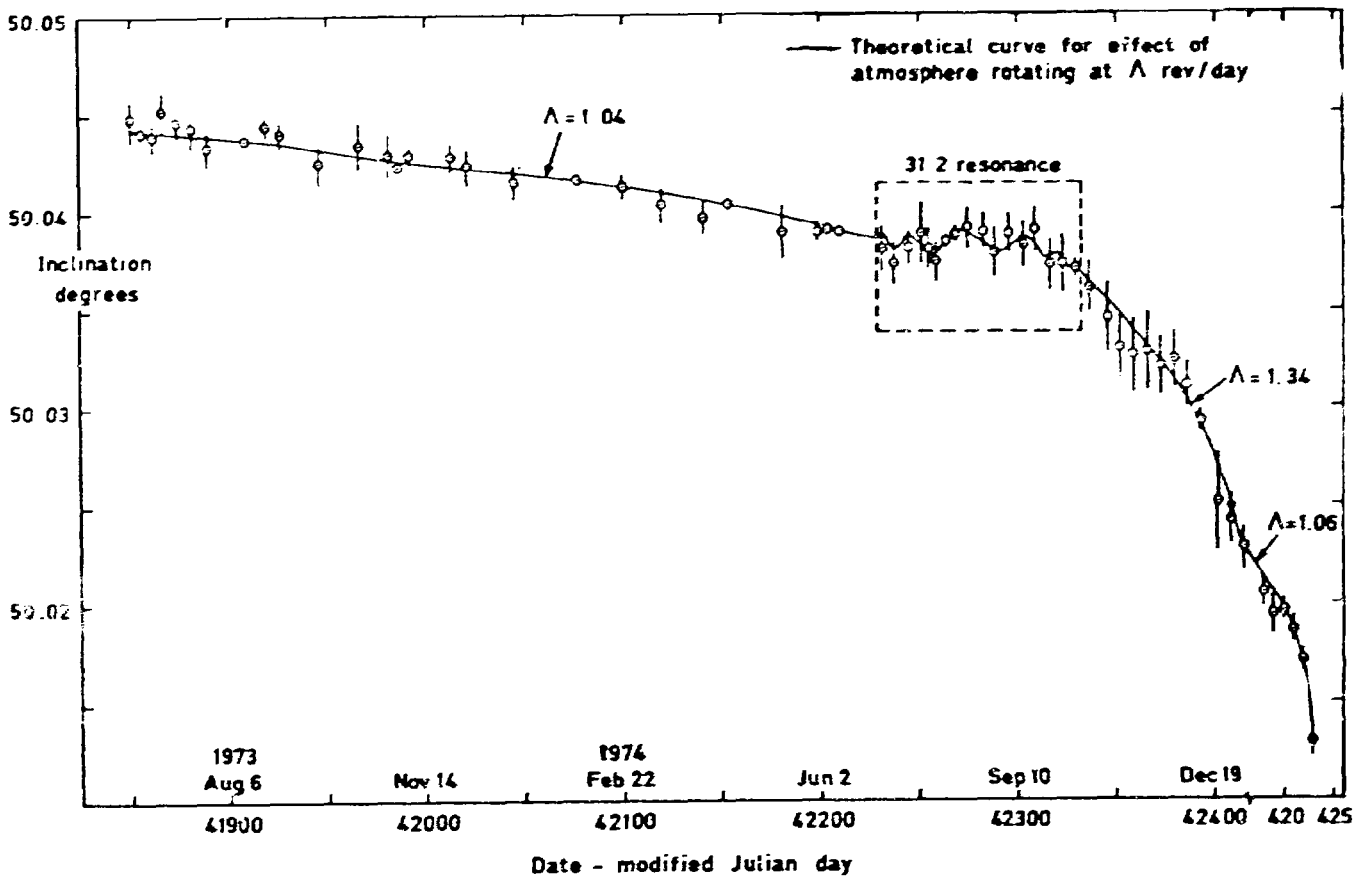

Fig 6 Values of inclination cleared of lunisolar, zonal harmonic and $J_{2,2}$ perturbations

Fig 6

Fig 7

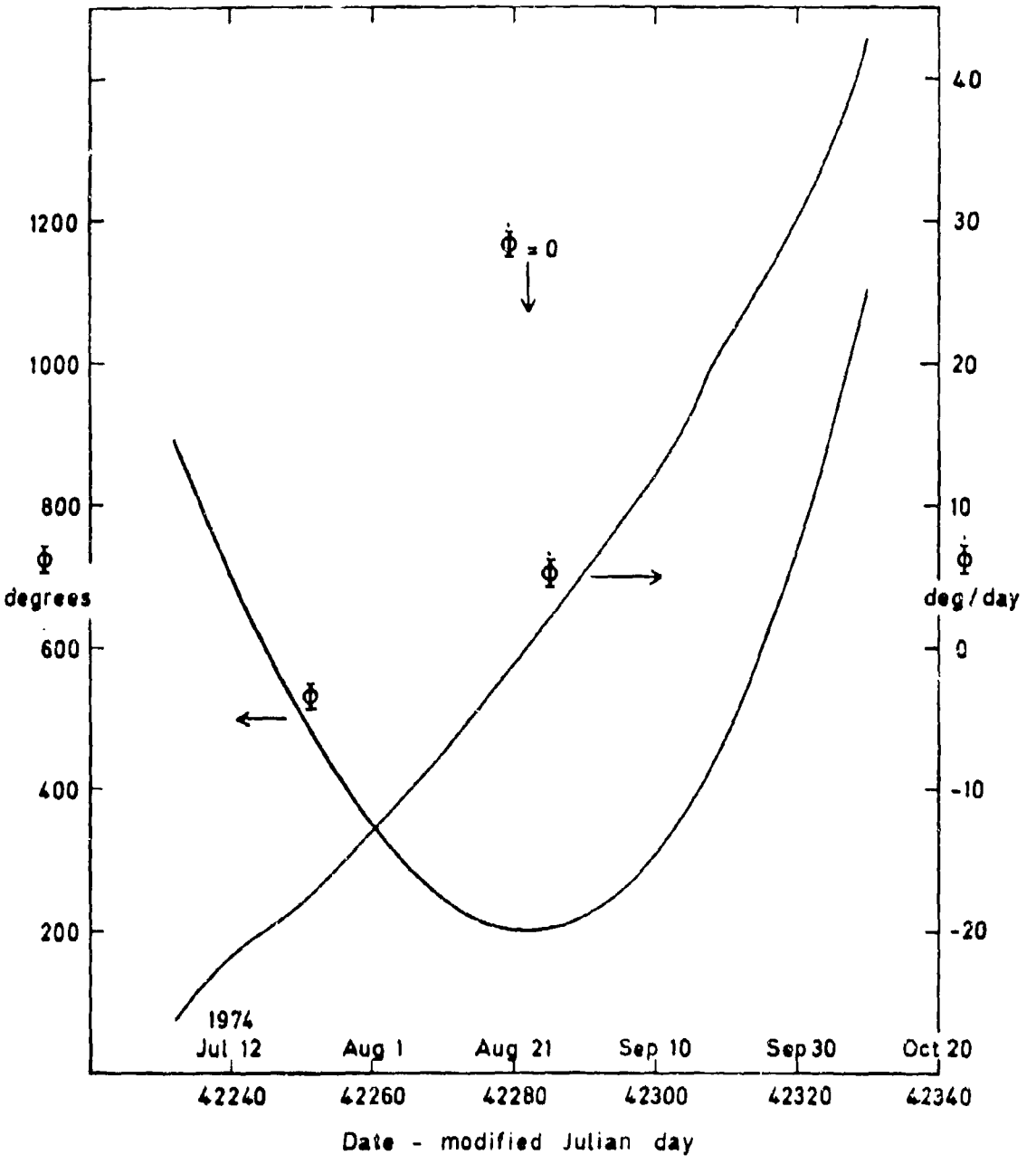

Fig 7 Variation of Φ and $\dot{\Phi}$ near 31:2 resonance

TR 79044

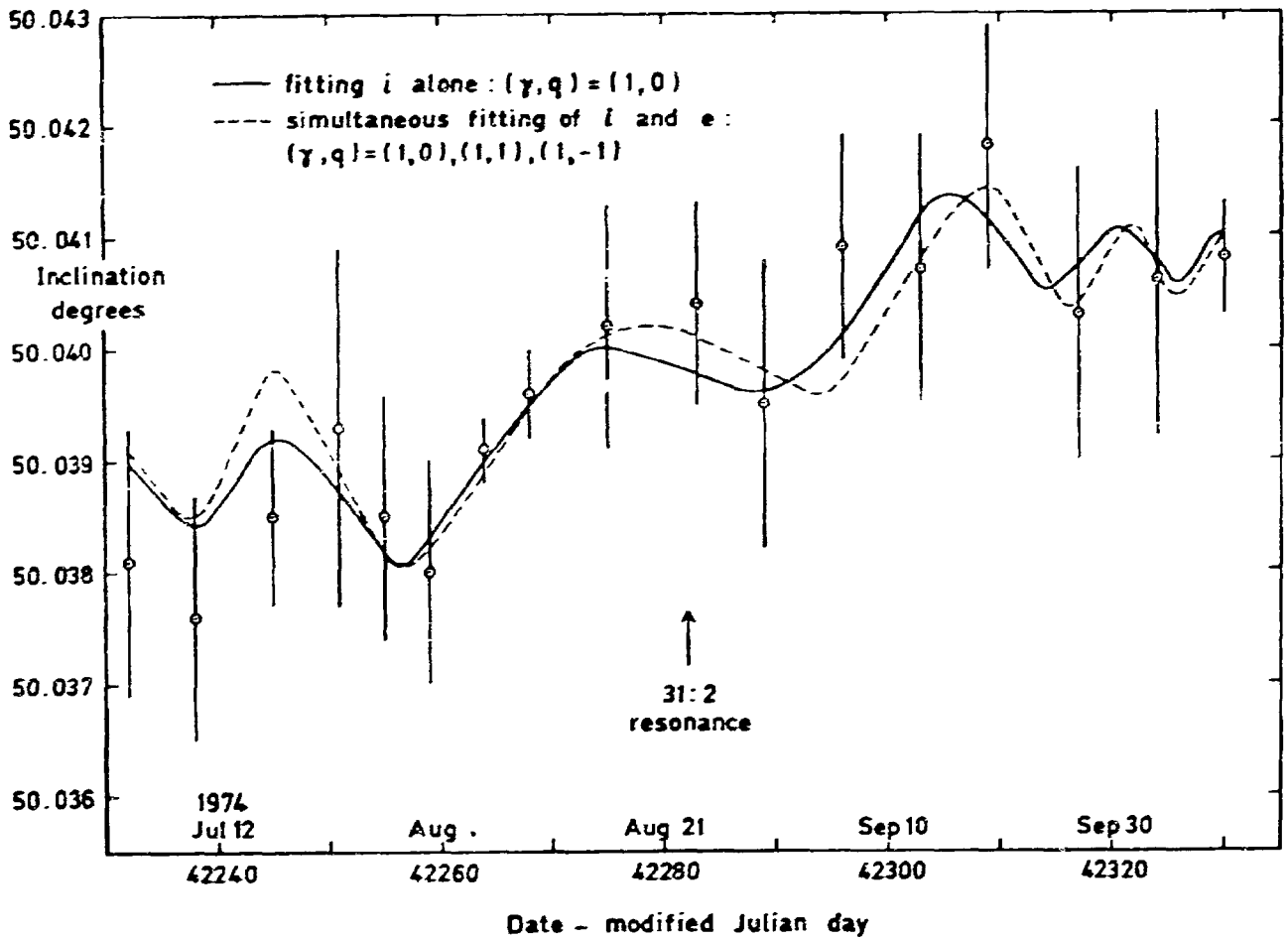

Fig 8 Values of inclination near 31:2 resonance, cleared of perturbations, with fitted theoretical curves

Fig 8

Fig 9a&b

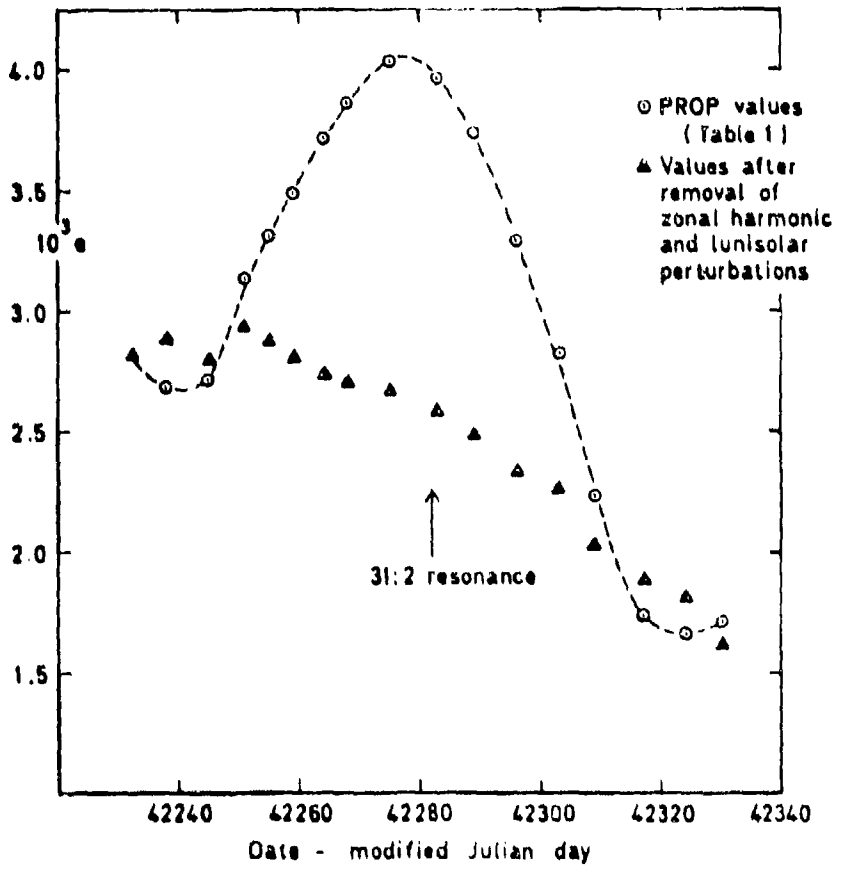

a PROP values and values cleared of gravitational perturbations

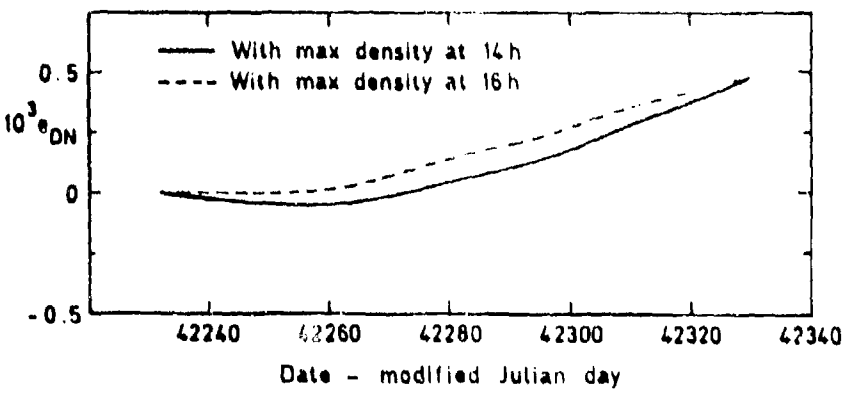

b The correction e_{DN} for the day-to-night variation in air density

Fig 9a&b Treatment of eccentricity around resonance

TP 79044

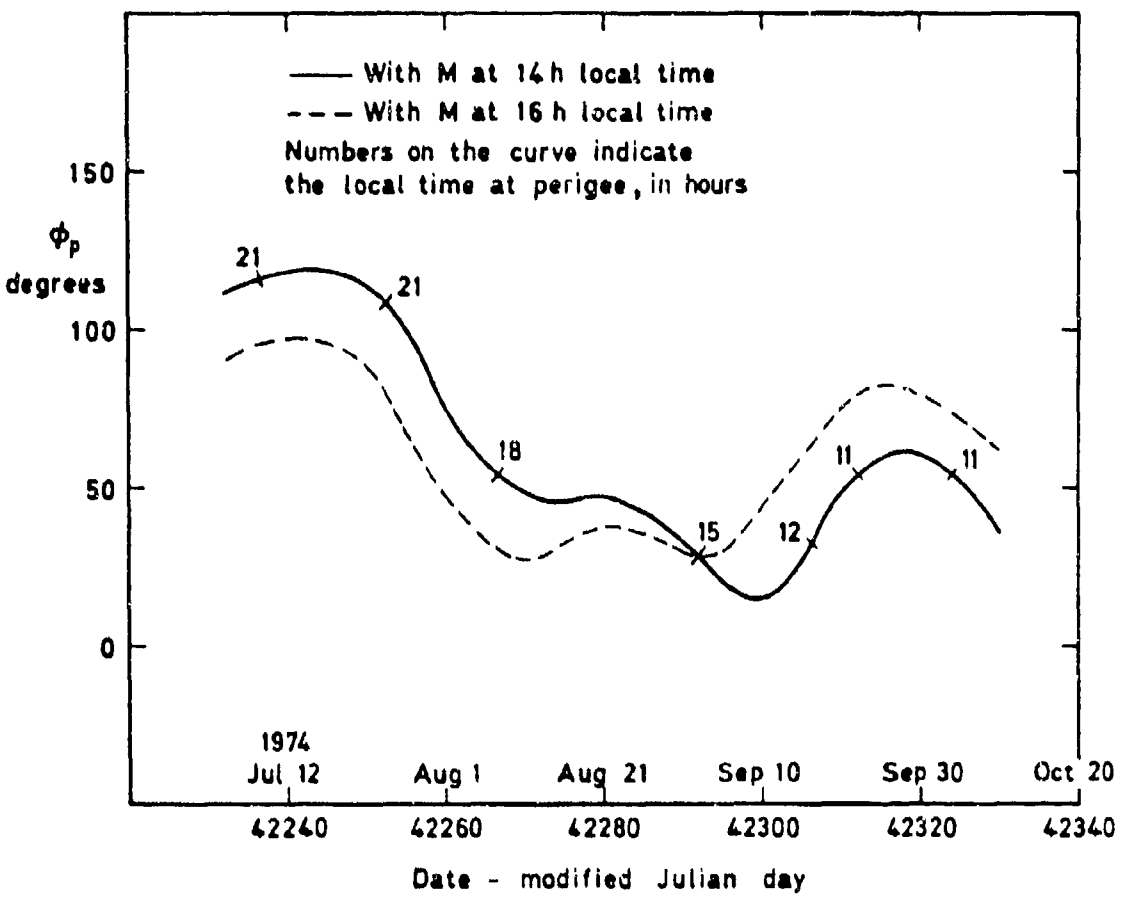

Fig 10 Variation near resonance of ϕ_p, the geocentric angle between perigee and the point M of maximum density

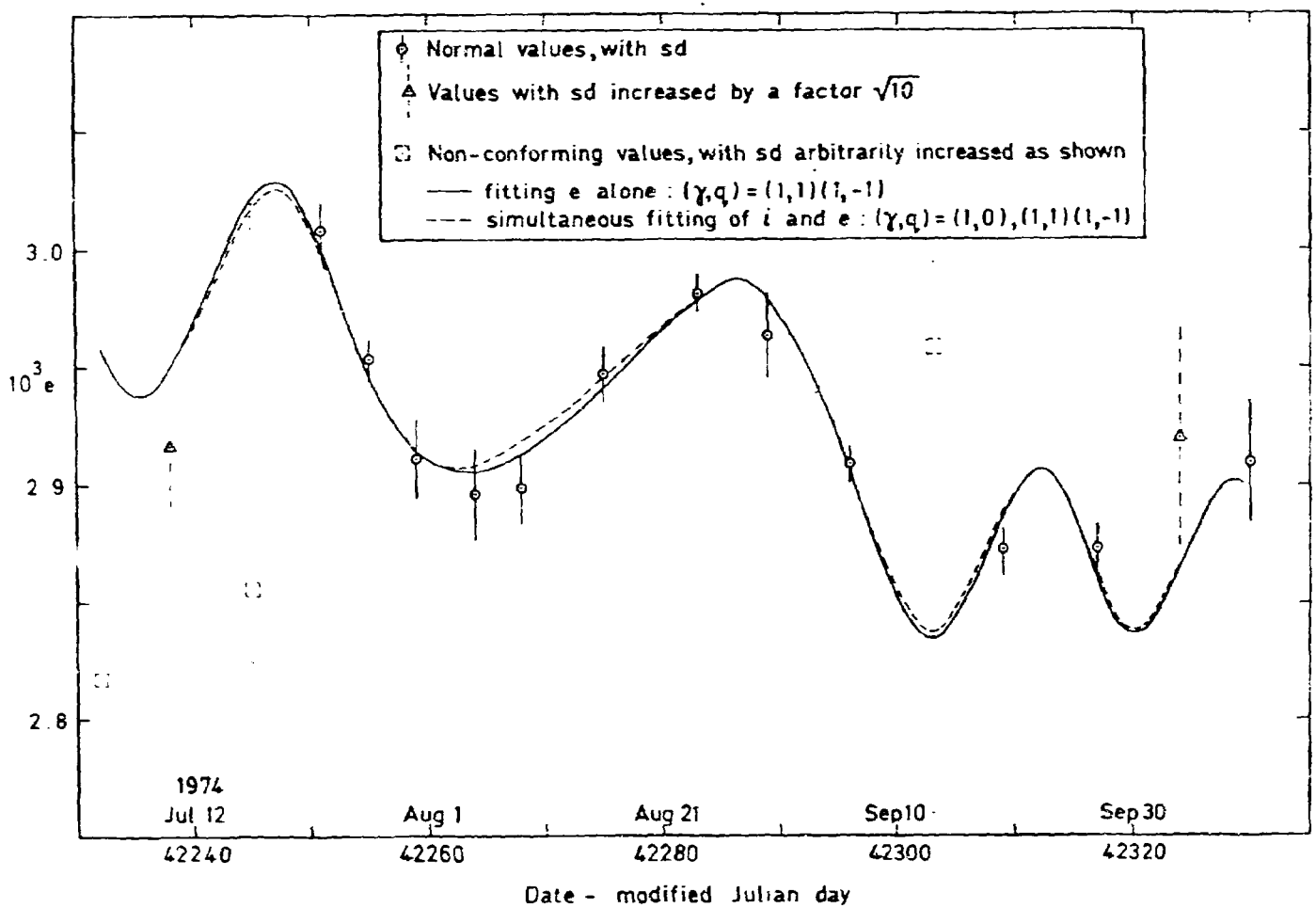

Fig 11 Values of eccentricity near 31:2 resonance, cleared of perturbations, with fitted theoretical curve

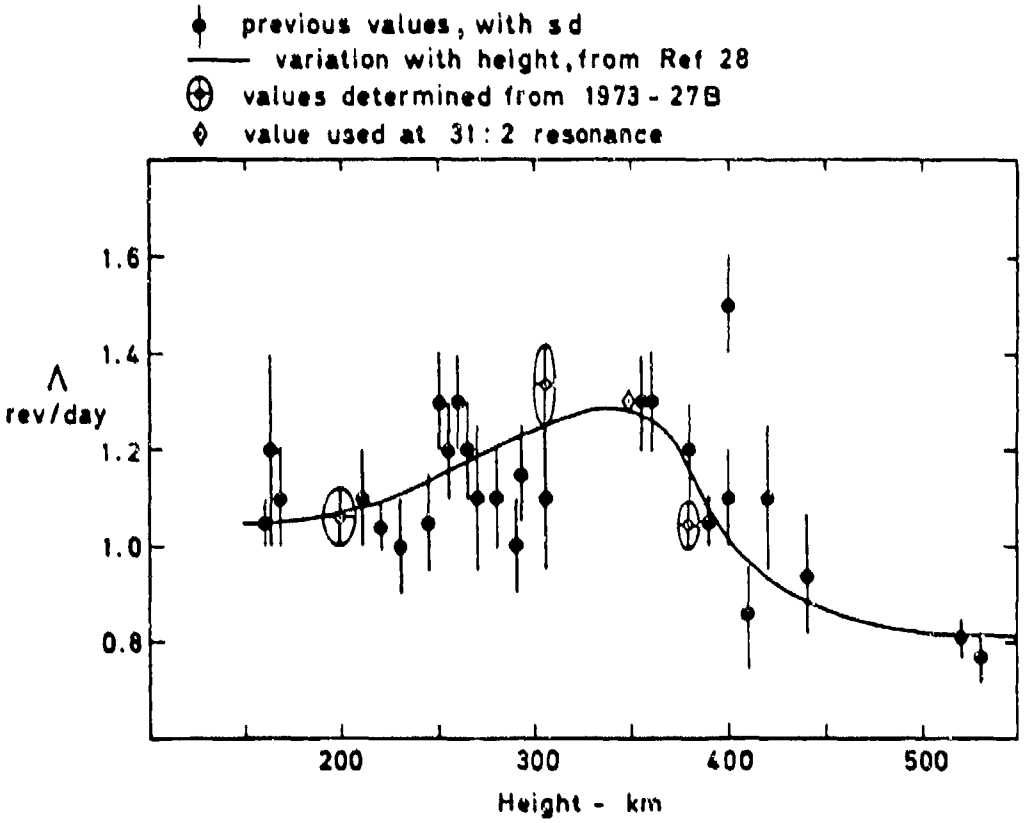

Fig 12 Previous values of mean atmospheric rotation rate, Λ, and new values from 1973-27B

Fig 13

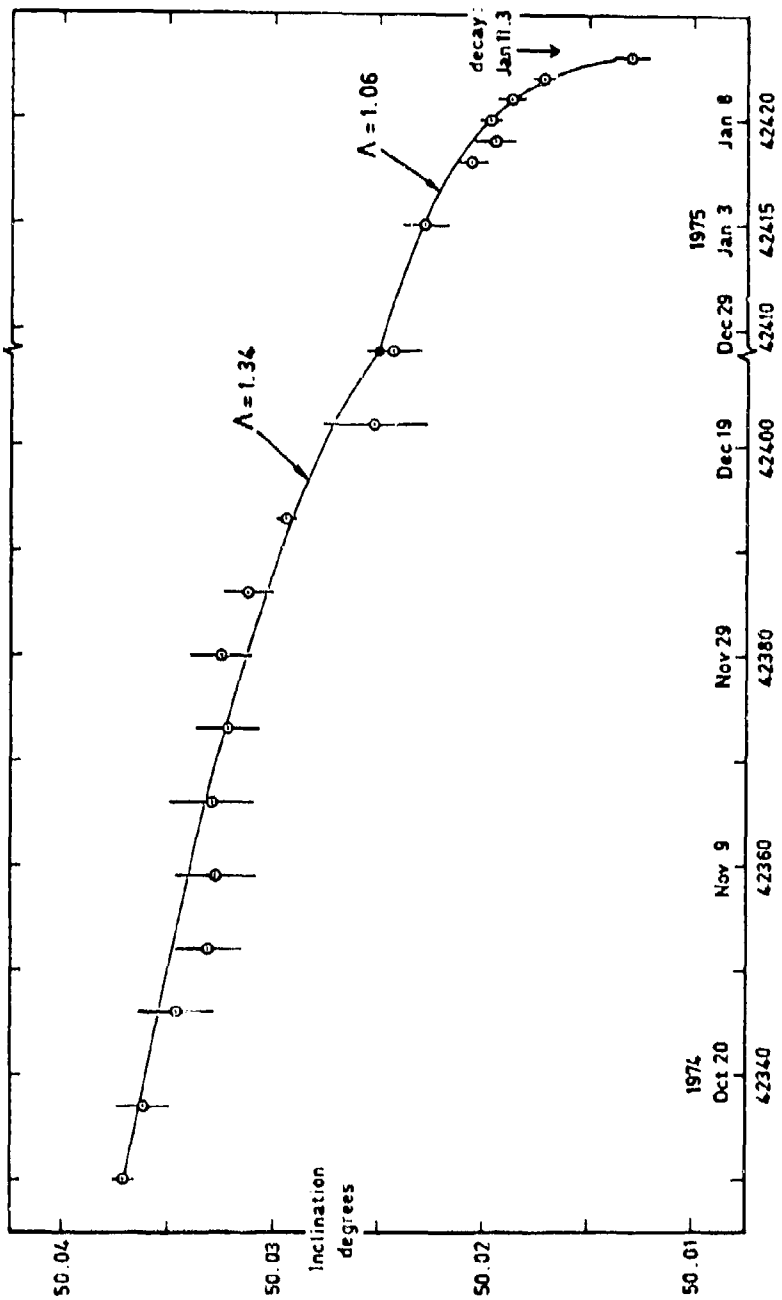

Fig 13 Values of inclination, cleared of gravitational perturbations, between 10 October 1974 and decay

TR 79044

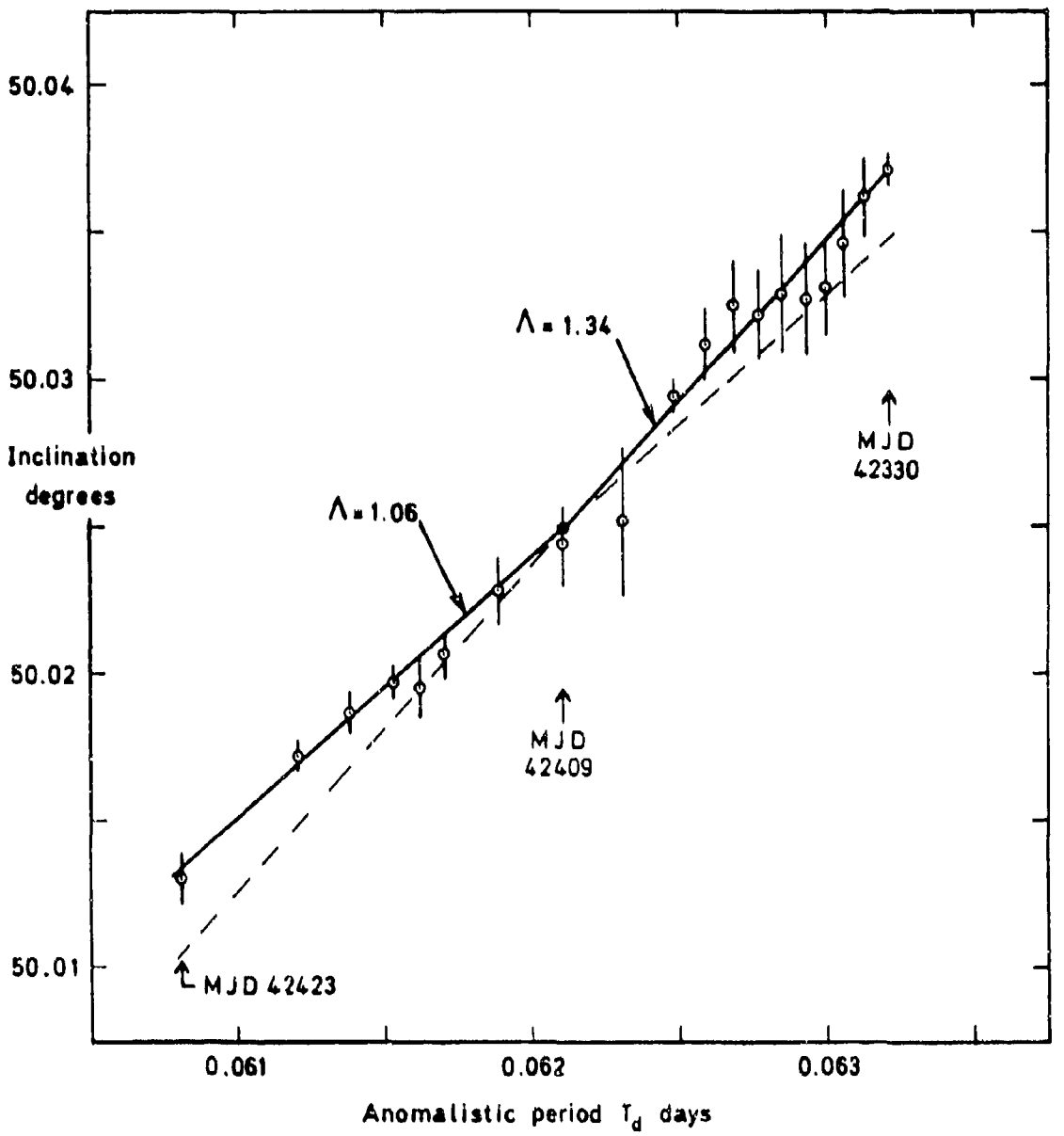

Fig 14 Values of inclination from Fig 13, plotted against orbital period

Fig 15

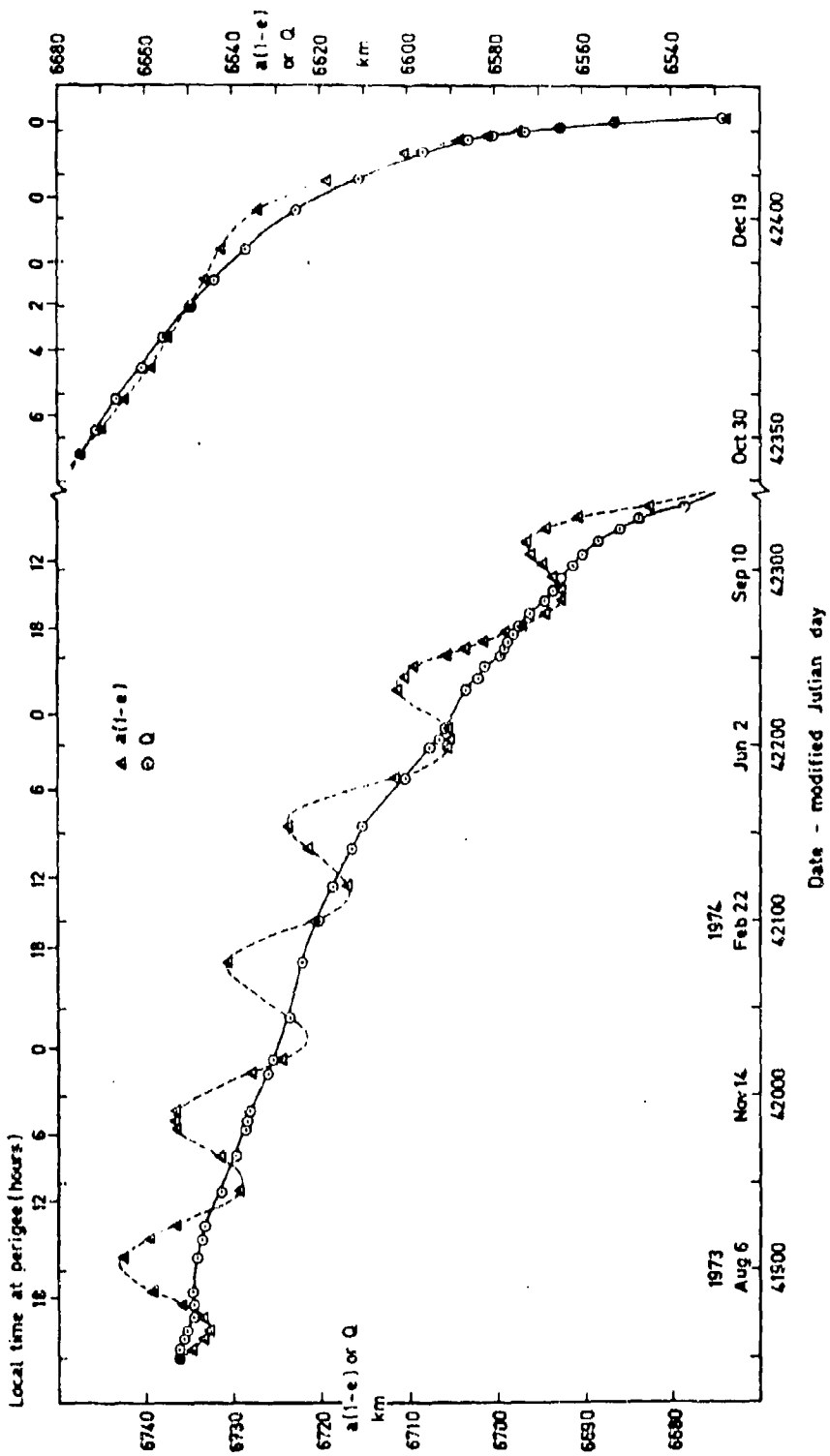

Fig 15 Values of a(1 – e) and Q

TR 79044

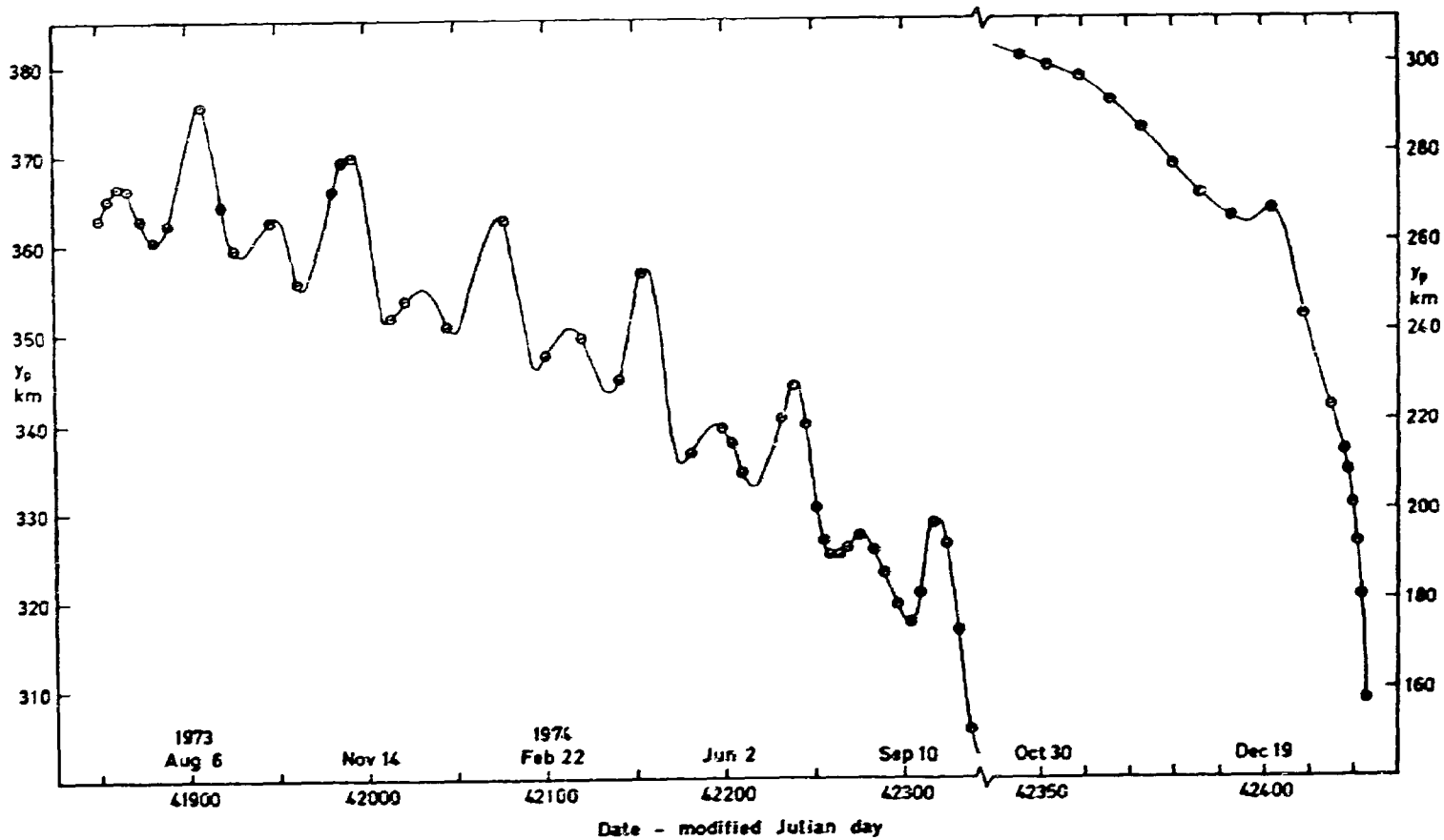

Fig 16 Values of perigee height y_p on the 62 orbits

Fig 17

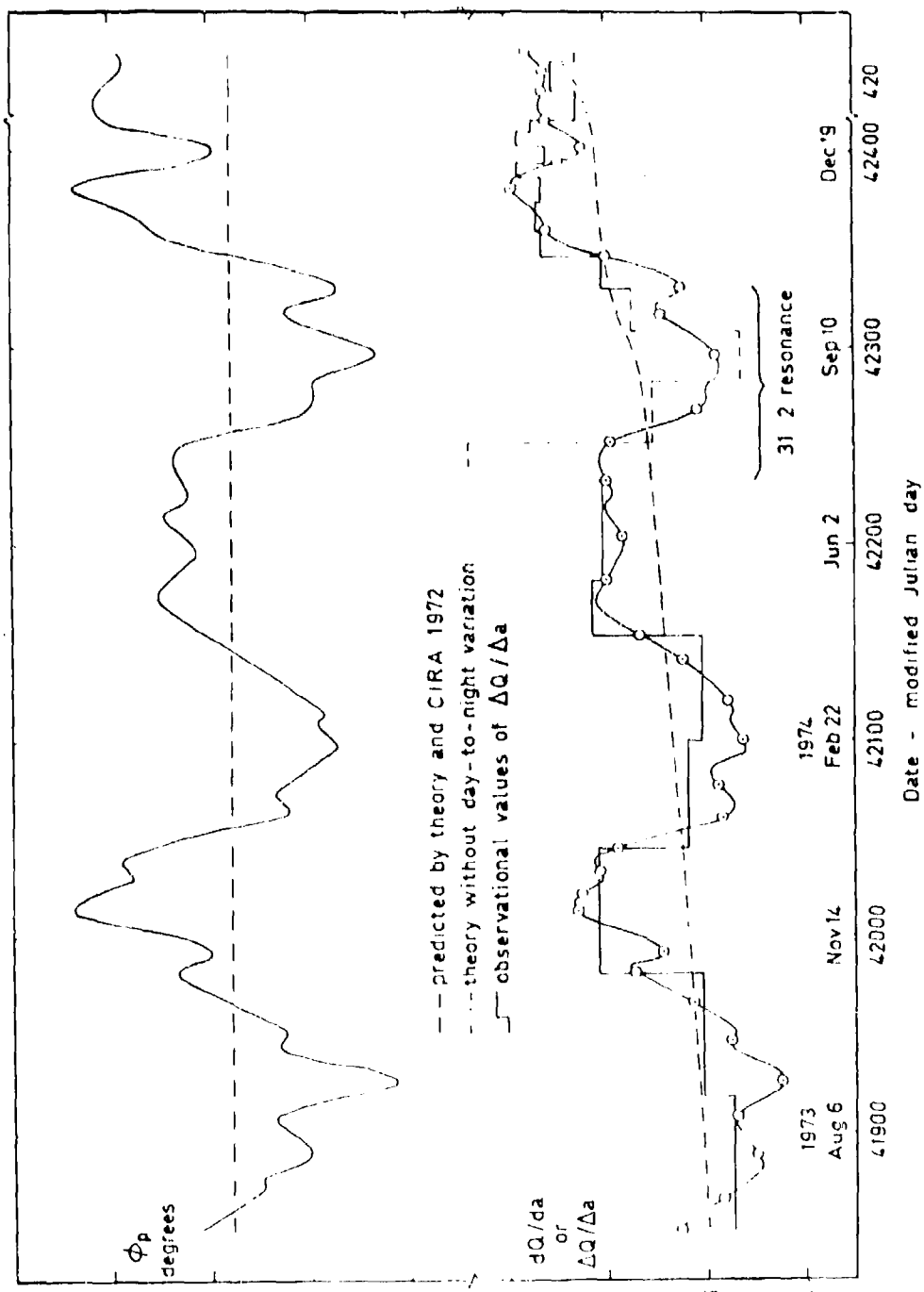

Fig 17 Thecretical values of dQ/da compared with observational values of ΔQ/Δa

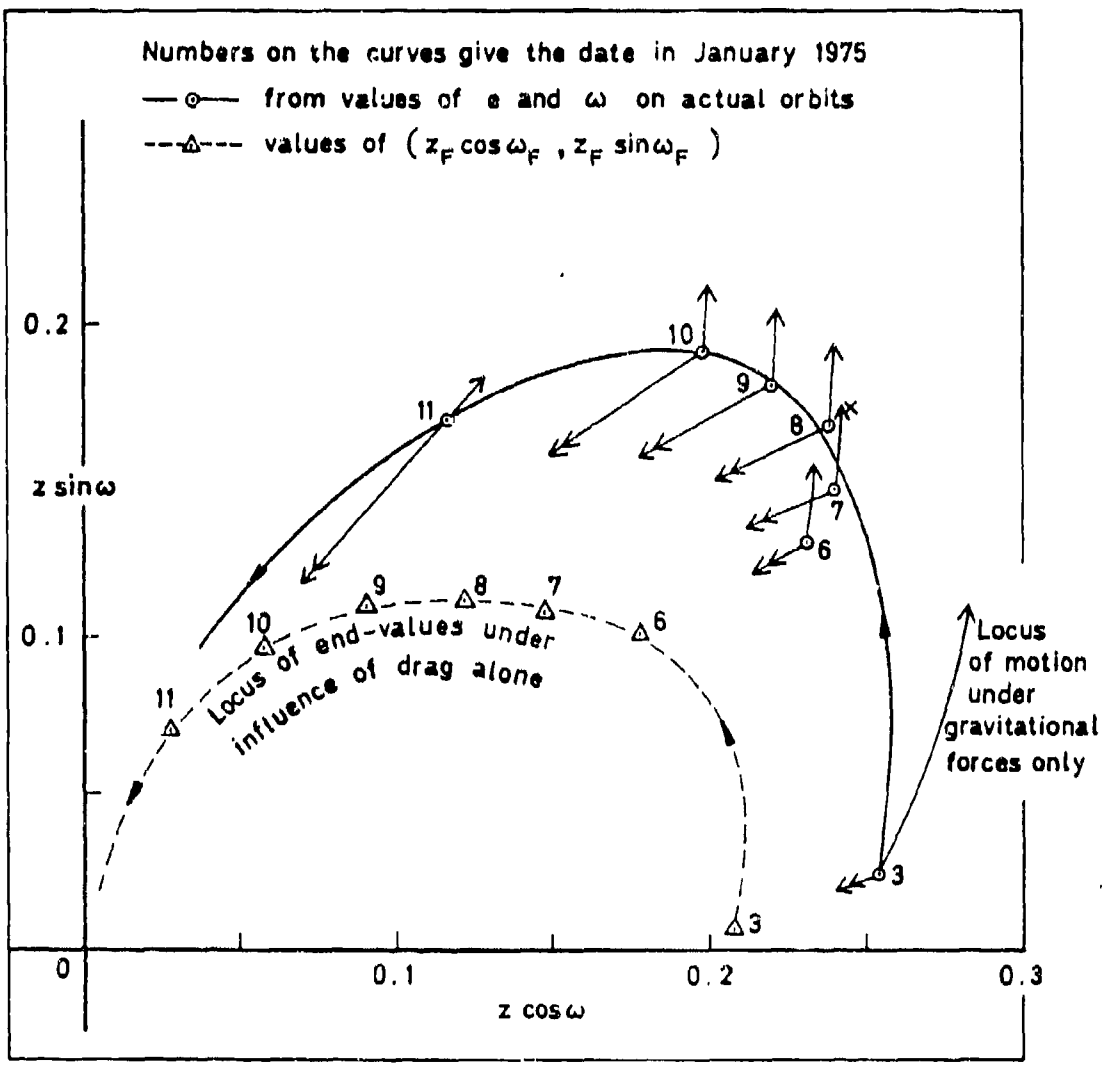

Fig 18 Variation of z and ω in the last 8 days of the life, 3-11 January 1975

Fig 19

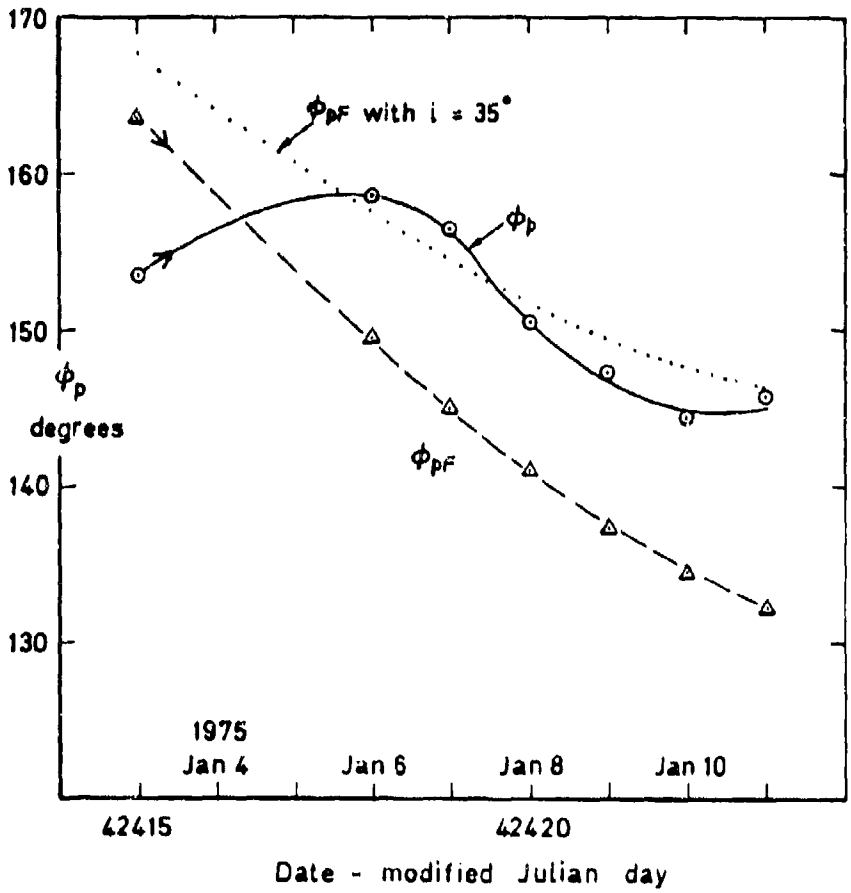

Fig 19 Values of ϕ_p and ϕ_{pF} near decay

REPORT DOCUMENTATION PAGE

Overall security classification of this page

UNCLASSIFIED

As far as possible this page should contain only unclassified information. If it is necessary to enter classified information, the box above must be marked to indicate the classification, e.g. Restricted, Confidential or Secret.

1. DRIC Reference (to be added by DRIC)	2. Originator's Reference	3. Agency Reference	4. Report Security Classification/Marking
	RAE TR 79044	N/A	UNCLASSIFIED

5. DRIC Code for Originator	6. Originator (Corporate Author) Name and Location
7673000W	Royal Aircraft Establishment, Farnborough, Hants, UK
5a. Sponsoring Agency's Code	6a. Sponsoring Agency (Contract Authority) Name and Location
N/A	N/A

7. Title Skylab 1 rocket, 1973-27B: orbit determination and analysis

7a. (For Translations) Title in Foreign Language

7b. (For Conference Papers) Title, Place and Date of Conference

8. Author 1. Surname, Initials	9a. Author 2	9b. Authors 3, 4	10. Date	Pages	Refs.
King-Hele, D.G.			April 1979	67	32

11. Contract Number	12. Period	13. Project	14. Other Reference Nos.
N/A	N/A		Space 564

15. Distribution statement

(a) Controlled by -- Head of Space Department (RAL)

(b) Special limitations (if any) -

16. Descriptors (Keywords) (Descriptors marked * are selected from TEST)

Skylab. Orbital theory. Orbit determination. Upper atmosphere winds. Earth's gravitational field.

17. Abstract

The final-stage rocket which projected Skylab into orbit on 14 May 1973 itself entered a nearly circular orbit at a height near 400 km, inclined at 50° to the equator. The rocket, designated 1973-27B, remained in orbit until 11 January 1975 and, being 25 m long and 10 m in diameter, was the brightest of the artificial satellites then visible. Its orbit has been determined at 62 epochs from some 5000 optical and radar observations. The average orbital accuracy in perigee height and orbital inclination is 90 m, though some orbits with Hewitt camera observations have much smaller sd (down to 10 m).

As the orbit contracted under the influence of air drag, it passed slowly through the 31:2 geopotential resonance, when the track over the Earth repeats every 31 revolutions at intervals of 2 days. The variations in inclination and eccentricity during the resonance phase have been analysed to determine values for six lumped 31st-order harmonic coefficients in the geopotential; these will provide a crucial test of the accuracy of future geopotential models.

The variation in inclination before and after resonance has been analysed to determine the average atmospheric rotation rate Λ (rev/day). Results are: $\Lambda = 1.04 \pm 0.05$ at height 380 km between June 1973 and June 1974; $\Lambda = 1.34 \pm 0.09$ at height 305 km for October-December 1974; and $\Lambda = 1.06 \pm 0.06$ at height 200 km in January 1975.

FS910/1

RAE Form A143